

Freie Universität Berlin, Institut für Geowissenschaften,
Section Paleontology
Malteserstrasse 74-100, 12249 Berlin

To
Editor Biogeosciences
Natascha Töpfer
Copernicus Publications

Dr. Jens Zinke
Sektion Paläontologie
12249 Berlin

Telefon +49 30 838-61034
Fax +49 30 838-70745
E-Mail jzens.inke@fu-berlin.de
Internet www.fu-berlin.de

04.10.2016

Revision bg-2016-69

Dear Editor,

Please find enclosed our final corrections for manuscript bg-2016-69 entitled "A sea surface temperature reconstruction for the southern Indian Ocean trade wind belt from corals in Rodrigues Island (19°S, 63°E)", for publication in Biogeosciences.

We thank both reviewers and you as Editor for the constructive comments that helped us to improve the manuscript and the acceptance of our paper. Below, you will find our detailed response to the specific comments by reviewer 1.

We sincerely hope that our revised manuscript is now suitable for publication in Biogeosciences.

Kind regards,
Jens Zinke

Answer to Specific comments:

Line 62: 'Synchronously'

Done.

Line 64: Figure 1b referenced but Figure 1a should come first.

Corrected.

Line 92: 'coral paleo-thermometers'

Done.

Line 93: 'alteration'

Done.

Line 99: 'Subtropical'

Done.

Line 154: 'occurring mostly'

Done.

Line 176: 'Fig. 1a'

Done.

Line 176-177: 'colony'

Done.

Line 179: 'August 2005 from a colony on the.....'

Done.

Line 181: 'March 2007 from a colony growing.....'

Done.

Line 191: 'Figs. A4 and A5' – should be relabelled/re-ordered in SM as Fig. A1 and Fig. A2 – as first occurrence in text.

Corrected.

• OK just realised my confusion between material presented in an Appendix and Supplementary material. Should these not be combined into one Supplementary Material file to prevent other readers being similarly confused.

We like to keep the Appendix figures separated from the Supplements because we feel that the Appendix figures provide important detail. The journal allows for Appendix figures to be separated from Supplements.

Line 191: 'coral density was calculated'

Done.

Line 196: 'samples for geochemical analysis'

Done.

Lines 202-204: 'Corals that showed an.....'; given there are only 2 corals, do the authors mean sections of corals?

Corrected.

Line 271-208: 'along the geochemical sampling tracks'

Done.

Line 221: 'was dissolved'

Done.

Line 222: 'was diluted'

Done.

Line 250: 'extracted various SST and....'

Done.

Line 251: 'for comparison with'

Done.

Line 257: HadISST is not listed in Table A1

Corrected.

Line 264: HadSST3 also not listed in Table A1

Corrected.

Line 269: HadMAT1 and HadnMAT2 not listed in Table A1

Corrected.

Line 273: Section 3 Materials and Methods should also include a description of the statistical analyses undertaken; the section should also include the description and data sources of the climate indices used (e.g. SIOD, PDO, ENSO) and other proxy coral records used.

Now included.

Line 282: 'between the two colonies'

Done.

Line 283: As Figure 2a presents Sr/Ca monthly anomalies, it is not possible to see the 'distinct seasonality' referred to in the text.

Corrected.

Line 288: anomalies 'higher' than what?

Relative to 1961-1990, now indicated.

Line 291: 'seasonality' not evident in Fig. 2a
Corrected.

Lines 309-310: Figure 4 does not show a radiograph
Corrected.

Line 312: 'and therefore the reported...'
Done.

Lines 334-335: Explain why just these 3 data sets were used for calibration.
Now reads "since SST seasonality does not differ significantly between SST products for the 2002 to 2006 period"

Lines 351-406: Section 5.4 – I still find this section extremely hard to follow and identify the key findings of the authors.

Without clearer definition what is hard to follow we cant address this point.

Line 406: I think that part of section 6.1 should appear in the Results rather than the Discussion. Need to clearly separate the findings of the study from discussing their implications etc.

We do not agree.

Line 410: Reference to Figures 7 and 8 in text before Figure 6.
Changed order of Figures.

Line 415: 'shows significant positive'; elsewhere referring to correlations indicated whether significant.

Done.

Lines 436-437: Figure 9 does not appear to show the Reunion Island record referred to.
Corrected.

Line 478: First reference to Figure 6 in text!
Order of Figures changed.

Line 481: 'very low overall density' – compared to what?
"compared to pre-1984 record" added

Line 506: 'new cores need to be obtained.....'
Done.

Line 844: 'density'
Done.

Line 989: 'inverted' rather than 'converted'

Done.

Lines 1000-1009: Please clarify labelling and caption to make it clear to reader which core sample is represented in each panel (e.g. Totor or Cabri).

Corrected.

Line 1030: How was this image of the coral core obtained? Is it under UV light?

No, just image software with blue colour.

Pages 54 and 55: Are these really positive X-ray prints, they look more like X-ray negatives?

Corrected.

1 **A sea surface temperature reconstruction for the southern Indian**
2 **Ocean trade wind belt from corals in Rodrigues Island (19°S, 63°E)**

3

4 J. Zinke^{1,2,3,4}, L. Reuning⁵, M. Pfeiffer⁵, J. Wassenburg⁶, E. Hardman⁷, R. Jhangeer-
5 Khan⁷, Davies, G. R.⁸, C.K.C. Ng⁹, and D. Kroon¹⁰

6

7 ¹Division of Paleontology, Freie Universitaet Berlin, Malteserstrasse 74-100, Berlin,
8 12249, Germany

9 ²Department of Environment and Agriculture, Curtin University of Technology, Kent
10 Street, Bentley, WA6102, Australia

11 ³Australian Institute of Marine Science, Nedlands, WA 6009, Australia

12 ⁴School of Geography, Archaeology and Environmental Studies, University of
13 Witwatersrand, Johannesburg, South Africa.

14 ⁵Geological Institute, RWTH Aachen, Wuellnerstrasse2, 52056 Aachen, Germany

15 ⁶Institute for Geosciences, Johannes-Gutenberg-University Mainz, Johann-Joachim-
16 Becher-Weg 21, D-55128 Mainz

17 ⁷SHOALS Rodrigues, Rodrigues, Mauritius

18 ⁸Geology & Geochemistry, VU University Amsterdam, De Boelelaan 1085, 1081 HV
19 Amsterdam, Netherlands

20 ⁹Department of Medical Radiation Sciences, Curtin University of Technology, Kent
21 Street, Bentley, WA6102, Australia

22 ¹⁰University of Edinburgh, School of GeoSciences, The King's Buildings, West Mains
23 Road, Edinburgh EH9 3JW, UK.

25

26 **Correspondence to:** Jens Zinke, jens.zinke@gmail.com

27

28 **Abstract**

29 The western Indian Ocean has been warming rapidly over recent decades causing a
30 greater number of extreme climatic events. It is therefore of paramount importance to
31 improve our understanding of links between Indian Ocean sea surface temperature (SST)
32 variability, climate change, and sustainability of tropical coral reef ecosystems. Here we
33 present monthly-resolved coral Sr/Ca records from two different locations from
34 Rodrigues Island (63°E, 19°S) in the south-central Indian Ocean trade wind belt. We
35 reconstruct SST based on a linear relationship with the Sr/Ca proxy with records starting
36 from 1781 and 1945, respectively. We assess relationships between the observed long-
37 term SST and climate fluctuations related to the El Nino-Southern Oscillation (ENSO),
38 the Subtropical Indian Ocean Dipole Mode (SIOD) and the Pacific Decadal Oscillation
39 (PDO) between 1945 and 2006, respectively. The reproducibility of the Sr/Ca records are
40 assessed as are the potential impacts of diagenesis and corallite orientation on Sr/Ca-SST
41 reconstructions. We calibrate individual robust Sr/Ca records with *in-situ* SST and
42 various gridded SST products. The results show that the SST record from Cabri provides
43 the first Indian Ocean coral proxy time series that records the SST signature of the PDO
44 in the south-central Indian Ocean since 1945. We suggest that additional records from
45 Rodrigues Island can provide excellent records of SST variations in the southern Indian
46 Ocean trade wind belt to unravel teleconnections with the SIOD/ENSO/PDO on longer
47 time scales.

48

49 **1 Introduction**

50 The Indian Ocean has been warming steadily over the past century with the western
51 portion of the basin having experienced an increase in SST of up to 1.2°C over the past
52 60 years (Koll Roxy et al., 2014). The Indian Ocean has also taken up a large amount of
53 heat in its interior between 1999 and 2016 when global SST increased at a smaller rate
54 compared to previous decades (Lee et al., 2015). The strong Indian Ocean warming over
55 the past century is thought to have contributed to a decreasing land-sea thermal contrast
56 with the Indian subcontinent affecting monsoon rainfall and potentially playing a major
57 role in the decrease in East African rainfall between March to May in recent decades
58 (Funk et al., 2008; Koll Roxy et al., 2015). The western Indian Ocean warming has also
59 been shown to follow closely anthropogenic radiative forcing over the past century (Funk
60 et al., 2008; Alory et al., 2009; Koll Roxy et al., 2015). Furthermore, the western Indian
61 Ocean warmed significantly during past El Niño events with the 1997/98 event causing
62 widespread coral bleaching and mortality (Sheppard, 2003). Synchronously, intrinsic
63 climate modes to the Indian Ocean, like the Subtropical Indian Ocean Dipole Mode
64 during austral summer (SIOD; Fig. 1a; Behera and Yamagata, 2001; Reason, 2001), can
65 interfere with the Indian Ocean-wide teleconnections in SST and rainfall caused by the El
66 Niño-Southern Oscillation (ENSO) or behave independently (Hoell et al., 2016).
67 Mounting evidence indicates that the Pacific Decadal Oscillation (PDO) or Pacific
68 Decadal Variability (PDV) has teleconnections extending to the western Indian Ocean
69 (Fig. 1b; Cole et al., 2000; Crüger et al., 2009). The positive PDO phase corresponds to
70 warm western Indian Ocean SST anomalies (Fig. 1b; Deser et al., 2004), thought to
71 exceed SST anomalies associated with ENSO (Krishnan and Sugi, 2003), particularly in

Jens Zinke 4/10/2016 4:17 PM

Deleted: b

Jens Zinke 4/10/2016 4:17 PM

Deleted: c

Jens Zinke 4/10/2016 4:17 PM

Deleted: c

75 the southwestern Indian Ocean (Meehl and Hu, 2006). It is therefore of paramount
76 importance to improve our understanding of links between Indian Ocean SST variability,
77 global climate change, and sustainability of tropical coral reef ecosystems. Yet, long-term
78 observational records of Indian Ocean SST are sparse and are thought to be only reliable
79 after the 1960's (Tokinaga et al., 2012).

80 Paleoclimate reconstructions of SST from massive corals have provided
81 invaluable records for past SST trends and interannual to decadal variability in the
82 western Indian Ocean (Charles et al., 1997; Cole et al., 2000; Cobb et al., 2001; Pfeiffer
83 et al., 2004, 2009; Pfeiffer & Dullo, 2006; Nakamura et al., 2009; Crueger et al., 2009;
84 Grove et al., 2013a, b; Zinke et al. 2008, 2009, 2014). Massive corals, such as *Porites*
85 spp., can grow for centuries at a rate of 0.5 and 2 cm.yr⁻¹. Therefore, down-core
86 geochemical sampling of massive corals can yield reconstructed SST time series at
87 approximately monthly resolution. As the coral precipitates its skeleton, trace elements
88 and stable isotopes are incorporated in proportion to ambient SSTs (Felis and Pätzold,
89 2003). Both, the Sr/Ca ratio and $\delta^{18}\text{O}$ composition of the coral aragonite have been shown
90 to be reliable paleo-thermometers with a negative relationship with SST (Alibert and
91 McCulloch, 1997; Pfeiffer & Dullo, 2006; DeLong et al., 2012). A compilation of Sr/Ca-
92 SST calibrations for *Porites* spp. revealed a mean Sr/Ca relationship with SST of -
93 0.061 mmol/mol/1°C SST increase (Corrège, 2006). Since Sr has a long oceanic residence
94 time, skeletal Sr/Ca is assumed to mainly reflect SST variability. The quality and
95 accuracy of coral paleo-thermometers strongly depends on optimal sampling of the major
96 growth axes (De Long et al., 2012). Furthermore, diagenetic alteration of coral aragonite
97 can lead to errors in SST reconstructions and it is important that this effect is identified

Jens Zinke 4/10/2016 2:56 PM
Deleted: s

99 and excluded based on petrographic analysis (McGregor and Gagan, 2003; Hendy et al.,
100 2007; McGregor and Abram, 2008; Sayani et al., 2011; Smodej et al., 2015).

101 Currently, none of the coral proxy records from the western Indian Ocean cover
102 the south-central Indian Ocean basin in the heart of the trade wind system and the
103 Subtropical Indian Ocean Dipole Mode (Fig. 1c). Furthermore, all proxy records of
104 interest for the trade wind belt are based on oxygen isotopes with the exception of two
105 Sr/Ca ratio records covering 1963 to 2008 from St. Marie Island off East Madagascar
106 (Grove et al., 2013a). The latter provided mixed results with discrepancies in terms of the
107 long-term SST trend estimates due to the confounding effects of coral calcification in at
108 least one core (Grove et al., 2013a). A coral oxygen isotope record from Reunion Island
109 (21°S, 55°E; Mascarene Islands) located approximately 230km to the southwest of
110 Mauritius spans the period 1832 to 1994 and is the longest for the subtropical region off
111 East Madagascar (Pfeiffer et al., 2004). Pfeiffer et al. (2004) showed evidence that the La
112 Reunion coral dominantly recorded past variation in salinity associated with transport
113 changes of the South Equatorial Current. The proxy time series records decadal
114 anomalies that were opposite to those of SST. Crüger et al. (2009) reported close linkages
115 of the salinity, sea-level pressure (SLP) and SST signal associated with the Pacific
116 Decadal Oscillation (Mantua et al., 1997) in coral records from Reunion and Ifaty (SW
117 Madagascar), respectively. Two coral oxygen isotope records from the Seychelles located
118 in the tropical western Indian Ocean (5°S, 54°E) were interpreted as an excellent record
119 of past Southwest Monsoon SST changes and showed significant correlations with air
120 temperatures over India between 1847 to 1994 (Charles et al., 1997; Pfeiffer & Dullo,
121 2006). Both, the Reunion and Seychelles records record strong correlations with the

Jens Zinke 4/10/2016 2:56 PM

Deleted: p

Jens Zinke 4/10/2016 4:17 PM

Deleted: b

124 ENSO on interannual and decadal time scales (Pfeiffer & Dullo, 2006). Although the
125 PDO also has a strong impact on the SST in the southwest Indian Ocean (Fig. 1c;
126 Krishnan and Sugi, 2003; Deser et al., 2004), the SST signature of the PDO has not
127 been reported in coral records from this region to date.

128 Here, we aim to reconstruct past SSTs from Sr/Ca ratios in two coral cores
129 obtained from Rodrigues Island (19°S, 63°E) located 690 km to the North-East of
130 Mauritius within the trade wind belt of the south-central Indian Ocean. To obtain a robust
131 SST record, we assess the reproducibility of the Sr/Ca proxy, and provide a rigorous
132 assessment of the potential impacts of diagenesis and corallite orientation on Sr/Ca-SST
133 reconstructions. We calibrate individual Sr/Ca records with *in-situ* SST and various
134 gridded SST products and verify the suitability of SST products for climate studies in the
135 south-central Indian Ocean. Furthermore, we assess relationships between the observed
136 long-term SST and climate fluctuations related to the ENSO ([Kaplan et al., 1998](#)), the
137 SIOD ([Behera and Yamagata, 2001](#)) and the PDO ([Mantua et al., 1997](#)) between 1945
138 and 2006, respectively.

139

140 **2 Regional setting and climate**

141 Rodrigues (63°E, 19°S) is a small volcanic island in the southern Indian Ocean, about
142 619 km east of Mauritius (Fig. 1c). It is part of the eastern edge of the Mascarene Plateau
143 that comprises Lower Tertiary basalts (Mart 1988) formed by a seaward flow of lava,
144 which has been eroded by hydrodynamic forces, and biological and chemical processes
145 (Turner and Klaus, 2005). Rodrigues has a surface area of about 119 km², with a
146 maximum altitude of 396 meter above sea level and is surrounded by a nearly continuous

147 fringing reef approximately 90 km in length (Turner and Klaus, 2005; Lynch et al. 2002).
148 The reef encloses a shallow lagoon, which, at 240km², is twice the area of the island
149 itself. The maximum tidal range is approximately 1.5m, and since the average water
150 depth in the lagoon is less than 2m, some areas are exposed at low spring tides. The water
151 depth immediately beyond the reef slopes is usually within the range of 10m to 30m. The
152 island has three major channels, one dredged for the main harbour at Port Mathurin in the
153 north, and natural channels in the south near Port Sud Est and in the East at St Francois.
154 Several small passes are also found around the reef (Turner and Klaus, 2005).

155 The water surrounding Rodrigues is supplied by the South Equatorial Current (SEC)
156 (New et al., 2005, 2007), a broad east to west current between 10° and 20° S in the Indian
157 Ocean driven by the southeast trade winds (Schott and McCreary, 2001). The southern
158 part of the SEC water flows in several directions past Rodrigues occurring mostly in
159 southwest and southeast direction, and westward to Mauritius (New et al., 2005, 2007).

160 Rodrigues has a relatively dry climate and annual mean evaporation exceeds
161 precipitation. Yearly precipitation is ~1000 mm mostly from January to April related to
162 the position of the Inter Tropical Convergent Zone (ITCZ). Between November and
163 March, the Southern Indian Ocean is affected by tropical cyclones, as a result of warm
164 SSTs and a strong convergence between northeast and southeast trades. Rodrigues
165 experiences two to sixteen cyclones per year, of which 2.5 are extreme (category 3 and
166 higher) with winds of 280 km/h and storm surges that reach 100 m inland and 2 m above
167 sea level. They usually last five to ten days (Turner and Klaus, 2005).

168 SST was monitored hourly *in situ* by a conductivity, temperature and depth (CTD)
169 device 150m offshore from the northern fringing reefs at Totor between 2002 to 2006

170 (Hardman et al., 2004, 2008). Maximum SST are recorded between December to March
171 ($28.6 \pm 0.5^\circ\text{C}$) and minimum SST between July to September ($22.4 \pm 0.27^\circ\text{C}$). Annual
172 mean SST is $25.49 \pm 0.24^\circ\text{C}$ with a seasonal amplitude of $6.22 \pm 0.68^\circ\text{C}$.

173 Air temperatures have been recorded by the WMO weather station 61988 (name:
174 Rodrigues, Mauritius) located at the northern coast of Rodrigues since 1951 and are
175 available at <http://climexp.knmi.nl/>. The most recent years between 1997 and 2007 have
176 been provided by the Rodrigues Meteorological Office. The warmest months are
177 December to March ($31.2 \pm 0.3^\circ$), the coldest months are July to September ($24.2 \pm 0.3^\circ$).
178 Yearly average air temperature is $27.49^\circ\text{C} \pm 0.31^\circ\text{C}$ with a yearly amplitude of about $7 \pm$
179 0.79°C .

180

181 **3 Materials and Methods**

182 Two coral cores were drilled from massive, dome-shaped *Porites* sp. and *Porites*
183 *lobata* at the northern reef sites Totor and Cabri, respectively (Fig. 1a; Table 1). The size
184 of the coral colony~~y~~ at Totor is $\sim 2.5\text{m}$ and that of Cabri is $\sim 4\text{m}$ in height. Both colonies
185 were healthy and showed no signs of disease or dead surfaces at the time of drilling. The
186 220cm long Totor core was obtained in August 2005 from a colony on the fore reef slope
187 of the northern fringing reef facing the open ocean with the top of the colony at 4m water
188 depth. The 180cm long Cabri core was obtained in March 2007 from a colony growing in
189 3m water depth about 1km to the northeast of Totor from the outer fringing reef at Passe
190 Cabri. The site Cabri is more exposed to trade winds as compared to Totor that is more
191 sheltered (Hardman et al., 2004, 2008).

Jens Zinke 4/10/2016 2:58 PM
Deleted: ies

193 A commercially available pneumatic drill driven by scuba tanks was used to
194 extract cores along the central growth axis, with a diameter measuring 4 cm. Cores were
195 sectioned into 7 mm thick slabs, rinsed several times with demineralised water, cleaned
196 with compressed air to remove any surficial particles and dried for more than 24 hours in
197 a laminar flow hood. Annual density bands were visualised by X-radiograph-positive
198 prints, and the growth axis of the coral slab was defined as the line normal to these
199 laminae (Figs. A1 and A2). Coral density g/cm^3 was calculated by analysing digital X-
200 rays using the program CoralXDS and densitometry (Fig. S1; Helmle et al., 2011;
201 Carricart-Ganivet et al., 2007), calcification rate ($\text{g}/\text{cm}^2 \text{ yr}^{-1}$) by multiplying density with
202 extension rate. The annual extension rates (cm yr^{-1}) were calculated by measuring the
203 distance (cm) between density minima using the program CoralXDS (Fig. S1). With a
204 diamond coated drill mounted on top of a movable support frame, samples for
205 geochemical analysis were taken every 1 mm parallel to the growth axis, equivalent to
206 approximately monthly resolution.

207 A combination of X-ray images, X-ray diffraction (XRD), light and scanning
208 electron microscopy (SEM) with Energy Dispersive X-Ray Spectrometer (EDS) was used
209 to investigate possible diagenetic alteration in the Totor and Cabri core sections. All core
210 sections from both Totor and Cabri were initially screened for diagenetic alterations using
211 X-ray images (Appendix Figs. 1 and 2). Core sections that showed an annual density
212 banding without anomalous high or low density patches were selected for further study
213 and considered free from obvious diagenetic alteration. Representative samples were
214 selected from both cores based on the X-ray images for SEM, thin-section and XRD
215 analysis. Additional samples were selected along the geochemical sampling tracks

Jens Zinke 4/10/2016 4:19 PM

Deleted: 4

Jens Zinke 4/10/2016 4:19 PM

Deleted: 5

Jens Zinke 4/10/2016 3:00 PM

Deleted: ies

Jens Zinke 4/10/2016 3:00 PM

Deleted: ere

Jens Zinke 4/10/2016 3:01 PM

Deleted: s

Jens Zinke 4/10/2016 4:19 PM

Deleted: 4

Jens Zinke 4/10/2016 4:19 PM

Deleted: 5

Jens Zinke 4/10/2016 3:01 PM

Deleted: als

Jens Zinke 4/10/2016 3:02 PM

Deleted: fter

Jens Zinke 4/10/2016 3:02 PM

Deleted: analysis

226 targeting intervals with unusually high or low Sr/Ca ratios. The powder-XRD
227 diffractometer at Rheinisch-Westfaelische Technische Hochschule (RWTH) Aachen
228 University was calibrated to detect and quantify very low calcite contents above \sim 0.2%
229 following the method of Smodej et al. (2015). In addition, the 2D-XRD system Bruker
230 D8 ADVANCE GADDS was used for XRD point-measurements directly on the coral
231 slab with a spatial resolution of \sim 4 mm and a calcite detection limit of \sim 0.2% (Smodej et
232 al., 2015). A 2-dimensional detector allows the simultaneous data collection over a large
233 2θ range, which reduces the counting time to 10 min for each sampling spot. The coral is
234 mounted on a motorized XYZ-stage and the position of each sample spot is controlled by
235 an automated laser-video alignment system. Multiple sample points can be predefined
236 and measured automatically. This method was used to test for the presence of secondary
237 calcite along the sampling traces of both corals.

238 Sr/Ca ratios were measured at the University of Kiel with a simultaneous
239 inductively coupled plasma optical emission spectrometer (ICP-OES, Spectro Ciros CCD
240 SOP; Zinke et al., 2014). Approximately 0.5mg of coral powder was dissolved in 1.00 ml
241 0.2M HNO₃. Prior to analysis, the solution was diluted with 0.2M HNO₃ to a final
242 concentration of \sim 8ppm Ca. An analogue in-house coral powder standard (Mayotte) was
243 analyzed after every six samples. The international reference material JCp-1 (coral
244 powder) was analyzed with every sample batch. All calibration solutions are matrix-
245 matched to 8 ppm Ca. Strontium and Ca are measured at their 407 and 317 nm
246 emission lines. Our intensity ratio calibration strategy combines the techniques described
247 by de Villiers et al. (2002) and Schrag (1999). Analytical precision of Sr/Ca

Jens Zinke 4/10/2016 3:03 PM
Deleted: are
Jens Zinke 4/10/2016 3:03 PM
Deleted: i

250 determinations as estimated from replicate measurements of unknown samples is 0.15%
251 or 0.01 mmol/mol (1sigma).

252 The coral core chronologies were developed based on the seasonal cycle of Sr/Ca.
253 We assigned the coldest month (either August or September) to the highest measured
254 Sr/Ca ratio (Sr/Ca maxima) in any given year, according to both *in situ* SST and grid-SST
255 (Extended reconstructed SST; Smith et al., 2008). We then interpolated linearly between
256 these anchor points to obtain age assignments for all other Sr/Ca measurements. In a
257 second step, the Sr/Ca data were interpolated to 12 equidistant points per year to obtain
258 monthly time series using AnalySeries 2.0 (Paillard et al., 1996). This approach creates a
259 non-cumulative time scale error of 1 - 2 month in any given year, due to interannual
260 differences in the exact timing of peak SST. The monthly interpolated Sr/Ca time series
261 were cross-checked with the chronologies from coral XDS to reveal the timing of high
262 and low density banding. High density bands in both corals formed in summer (low
263 Sr/Ca) of any given year.

264 We extracted coral proxy data for comparison to our Rodrigues time series from
265 the NOAA paleoclimate data archive ([https://www.ncdc.noaa.gov/data-](https://www.ncdc.noaa.gov/data-access/paleoclimatology-data/datasets/coral-sclerosponge)
266 access/paleoclimatology-data/datasets/coral-sclerosponge). We used the time series for
267 the Seychelles (Pfeiffer and Dullo, 2006), La Reunion (Pfeiffer et al., 2004) and St. Marie
268 Island (Grove et al., 2013).

269

270 **4 Historical SST data and climate indices**

271 Historical SST data collected primarily by ships-of-opportunity have been summarised
272 in the comprehensive ocean atmosphere data set (ICOADS) to produce monthly averages

273 on a 2x2° grid basis (Woodruff et al., 2005). In the grid that includes Rodrigues Island
274 the data are extremely sparse (Fig. A3). Since the uncertainty in SST bias adjustments
275 due to measurement errors is much larger for Southern Hemisphere than the Northern
276 Hemisphere (Jones, 2016) data, we therefore extracted various SST and marine air
277 temperature datasets for our region for comparison with our coral proxy data. We
278 extracted SST from extended reconstructed SST (ERSST version 3b/version 4; Smith et
279 al., 2008), also based on ICOADS data, which uses sophisticated statistical methods to
280 reconstruct SST from sparse data. From ERSST, we extracted data in the 2x2° grid
281 centred at 61-63°E, 19-21°S (Table A1). Furthermore, we used Met Office Hadley
282 Centre's sea ice and sea surface temperature (HadISST) data for the grid 62-63°E, 19-
283 20°S (Rayner et al., 2003; Kennedy et al., 2011). HadISST temperatures were
284 reconstructed using a two-stage reduced-space optimal interpolation procedure, followed
285 by superposition of quality-improved gridded observations onto the reconstructions to
286 restore local detail. Since January 1982, SST time series for HadISST use the optimal
287 interpolation SST (OISST; 1x1°), version 2 (Reynolds et al., 2002) that includes
288 continuous time series of satellite-based SST measurements. We also extracted Advanced
289 Very High Resolution Radiometer (AVHRR) SST at 0.25x0.25° resolution (Reynolds et
290 al., 2007; Tab. A1) from 1985 to 2006. SST from the 5x5° HadSST3, the most
291 sophisticated bias-corrected SST data to date, were downloaded for the region 60-65°E,
292 15-20°S (Kennedy et al., 2011) but contains data gaps throughout the record due to strict
293 quality control. SST is reported as anomalies relative to the 1961 to 1990 mean
294 climatology. In addition, we extracted 5x5° night-time marine air temperature data from
295 HadMAT1 and HadNMAT2 datasets (Kent et al., 2013). HadNMAT2 also contains data

Jens Zinke 4/10/2016 4:20 PM

Deleted: 1

Jens Zinke 4/10/2016 3:04 PM

Deleted: a large number of

Jens Zinke 4/10/2016 3:04 PM

Deleted: i

Jens Zinke 4/10/2016 3:04 PM

Deleted: n

Jens Zinke 4/10/2016 3:04 PM

Deleted: to

Jens Zinke 4/10/2016 3:06 PM

Deleted: ; Table A1

Jens Zinke 4/10/2016 3:06 PM

Deleted: ; Appendix Table 1

303 gaps throughout the record due to strict quality control. Night-time marine surface air
304 temperature is highly correlated with SST but free of the biases introduced by changes in
305 SST measurement techniques (Tokinaga et al., 2012).

306 All climate indices used for comparison with instrumental and coral proxy data were
307 extracted from the Royal Netherlands Meteorological Institute (KNMI) online tool
308 climate explorer (Trouet and Oldenborgh, 2005). We extracted the time series for the
309 Subtropical Indian Ocean Dipole Mode (SIOD; Behera and Yamagata, 2001), the El
310 Niño-Southern Oscillation (ENSO; Kaplan et al., 1998) and the Pacific Decadal
311 Oscillation (PDO; Mantua et al., 1997).

312 Statistical analysis includes linear correlation for linearly detrended data only with
313 climate indices and instrumental data with 95% confidence limits indicated for the
314 correlation coefficients using a Monte Carlo approach (Trouet and Oldenborgh, 2005; see
315 Supplementary Data). Spatial correlations for linearly detrended data only were computed
316 at knmi climate explorer (van Oldenborgh and Burgers, 2005) taking into account only
317 correlations with $p < 0.05$.

318

319 **5 Results**

320 **5.1 Coral Sr/Ca seasonality, variability and trends**

321 The average growth rate of the corals Totor (224 years) and Cabri (130 years)
322 were $9.82 \pm 0.19 \text{ mm y}^{-1}$ and $11.79 \pm 0.25 \text{ mm y}^{-1}$, respectively (Table 1; Fig. S1). The Cabri
323 core shows a growth disturbance at 1907 that led to partial colony mortality (see Suppl.
324 Information). This lower core section is overprinted by diagenesis and it is therefore not
325 suitable for climate studies or to determine density and calcification rates.

326 For the period of overlap (1945 to 2005) there is an offset in mean Sr/Ca of
327 0.0242 mmol/mol between the two colonies. Both cores show a distinct seasonality in
328 Sr/Ca throughout their record length. The seasonality in the Totor core (0.283±0.049
329 mmol/mol) is on average slightly higher compared to the Cabri core (0.238±0.055
330 mmol/mol), yet the difference is not statistically significant (both overlap within 1σ). To
331 eliminate the offset between Sr/Ca time series we calculated Sr/Ca anomalies by
332 subtracting their mean relative to the 1961 to 1990 reference period (Fig. 2a).

Jens Zinke 4/10/2016 3:32 PM

Deleted: (Fig. 2a)

333 Between 1945 and 2006 both cores record higher Sr/Ca anomalies relative to
334 1961-1990 (a period of cooling) that started in the mid 1950's and lasted until the early
335 1970's. Both cores show a pronounced trend to more negative Sr/Ca values (warming)
336 starting in the 1970's (Fig. 2a). After 1984 Sr/Ca in the Cabri core further decreases
337 (warms) while Sr/Ca in the Totor core records no trend. This highlights that the long-term
338 trend estimates after 1984 need to be viewed with caution.

Jens Zinke 4/10/2016 3:32 PM

Deleted: ure

339 The Sr/Ca time series in the Totor core extends to 1781 (Fig. 2a). Marked
340 negative Sr/Ca anomalies (warmer) are observed during the first half of the 20th century
341 centered at 1918/19, 1936-41 and in the period 1948-1951 that exceed anomalies in the
342 1961 to 1990 reference period. Sr/Ca anomalies between 1850 and 1890 are higher
343 (cooler) while decadal periods with lower (warmer) Sr/Ca are observed between 1781
344 and 1850 relative to 1961 to 1990.

Jens Zinke 4/10/2016 3:35 PM

Deleted: and reduced seasonality in that period

345
346 **5.2 Diagenetic tests for alterations of Sr/Ca profiles**

347 Representative samples for diagenetic screening with XRD, SEM and light
348 microscopy were identified on the coral slabs using the X-radiographs (Fig. A1 and A2).

353 Additionally, intervals with presumably anomalous proxy values (warm or cold
354 anomalies) were analyzed with the same methods. Ten thin-sections, six SEM samples,
355 ten powder-XRD and thirteen spot-2D-XRD samples were analyzed from coral core
356 Totor (Fig. 3). For coral core Cabri, seven thin-sections, one powder-XRD and six 2D-
357 XRD samples were analyzed. Neither powder nor spot-XRD analysis detected any
358 calcite. Thin-section analysis indicates a growth break within core section 12 of Totor
359 that is also apparent in the radiograph (Fig. A1). Close to this break the coral is strongly
360 affected by bioerosion and encrustation by red algae (Fig. 3e). The sampling transect for
361 geochemical analysis, however, excluded this area and therefore the reported data are not
362 affected by diagenesis. Combined SEM, EDS and XRD analysis shows low amounts of
363 patchy distributed isopachous ($\sim 2\mu\text{m}$) fibrous aragonite cement in Totor core section 6
364 (1916-1921), 7 (1882-1887) and 11 (~ 1809).

365 Aragonite cement should lead to higher Sr/Ca values and lower reconstructed
366 temperatures (Hendy et al., 2007). An interesting outcome is that the observed diagenesis
367 is not able to explain changes in the Sr/Ca ratios except for the Totor core section 7. Here
368 the observed aragonite cement is associated with relatively high Sr/Ca values resulting in
369 an apparent cold anomaly. No anomalously high Sr/Ca ratios are associated with the
370 patchy aragonite cements in Totor core sections 6 and 11. Instead core sections 6 and 11
371 are characterized by low Sr/Ca ratios resulting in apparent relatively warm reconstructed
372 temperatures. All other samples from the core sections Totor 3, 4, 8, 9 and 10 are devoid
373 of diagenetic alteration. In summary, a diagenetic influence on the proxy record and
374 resulting SST reconstructions are only evident for Totor core section 7 (years 1882-
375 1887). Core Cabri showed only localized (single month) positive Sr/Ca anomalies (cool

Jens Zinke 4/10/2016 3:38 PM
Deleted: Fig. 4; Appendix
Jens Zinke 4/10/2016 4:21 PM
Deleted: 5
Jens Zinke 4/10/2016 3:38 PM
Deleted: is
Jens Zinke 5/10/2016 10:29 AM
Deleted: (Fig. 8e)

380 SST bias; Fig. 3f). Thin-section and XRD analysis did not establish any diagenetic
381 alteration, but the coral locally contained aragonitic sediment partially filling pore spaces
382 (Fig. 3f). This aragonitic sediment potentially could have caused the isolated Sr/Ca peaks
383 (high Sr/Ca) in the record. These individual data points were omitted from further
384 analysis.

385

386 **5.3. Calibration of coral Sr/Ca-SST with in-situ and gridded SST**

387 SST seasonality does not differ significantly between SST products for the 2002
388 to 2006 period for which we had *in situ* SST. Therefore, the coral Sr/Ca from both cores
389 was calibrated with *in situ* SST, ERSSTv.3b and AVHRR SST for the period 2002 to
390 2006 using the minima and maxima in any given year, as well as monthly values with
391 AVHRR SST for 1981 to 2006 (Fig. 4; Tab. A2). There is a relatively large variance in
392 the Sr/Ca-SST relationships depending on the coral core and the SST record. The slopes
393 of the ordinary least squares regressions vary between -0.0384 to -0.0638 mmol/mol per
394 1°C (Tab. A2). The lowest slopes are obtained with *in situ* SST and the highest with
395 ERSSTv.3b (Tab. A2). The range of this variance is consistent with the results of Corrège
396 (2006), who used a set of more than 30 coral Sr/Ca records from various ocean basins and
397 different coral genera. We reconstructed absolute SST for the period of overlap with *in*
398 *situ* SST from 2002 to 2006 from both coral cores (Fig. 4). The Sr/Ca-SST in the Totor
399 core shows the best fit with *in situ* SST in terms of the seasonal amplitude. The Sr/Ca-
400 SST in the Cabri core overestimates the winter SST of 2002 and 2005, yet agrees well for
401 2003 and 2004 (Fig. 4). Taking into account the uncertainties (measurement error,

Jens Zinke 5/10/2016 10:32 AM
Formatted: Font:Italic

Jens Zinke 4/10/2016 3:41 PM
Deleted: (Fig. 4; Tab. A2).

403 regression error) in absolute SST from Sr/Ca for Cabri and Totor of 1.23°C and 1.05°C
404 (1 σ), respectively, the coral data agree with *in situ* SST within the 1 σ uncertainty.

405

406 **5.4. Validation of Sr/Ca-SST anomalies with gridded SST products**

407 To eliminate errors associated with absolute SST reconstructions from coral Sr/Ca
408 we calculated relative changes in SST for the coral temperature records relative to the
409 1961 to 1990 mean based on the established empirical relationship of -0.0607 mmol/mol
410 per 1°C derived from >30 published Sr/Ca calibrations (Corrège, 2006; Nurhati et al.,
411 2011). This slope is well within the range of our regressions based on a variety of SST
412 datasets and consistent with the results of Corrège (2006). (Tab. A2). We consider the
413 mean Sr/Ca-SST slope of Corrège (2006) to be much more reliable than our short *in situ*
414 calibration. We use a conservative estimate of the uncertainty around relative SST
415 changes based on the difference between lower (-0.04) and upper slope (-0.084) estimates
416 from these regression equations, thus ± 0.02 mmol per 1°C or ± 0.33 °C (following Gagan
417 et al., 2012; Tab. A2).

418 We validated the coral derived annual mean SST reconstruction against local Air
419 Temperature (AT), ERSSTv3b, ERSST4, HadISST, HadSST3, HadMAT1 and
420 HadNMAT2 for the period 1951 to 2006 (Fig. 5; See Supplementary Tables 1-16 for
421 mean annual correlations). We stress that the number of SST observations in the
422 ICOADS SST and marine AT database is extremely sparse for our region (Fig. A3). The
423 Cabri coral SST record records the highest correlations with HadISST and HadMAT1 in
424 the grid box surrounding Rodrigues Island (Fig. A4) while the overall best fit is obtained
425 with local Rodrigues AT. Core Totor has no significant correlations with both ERSST

Jens Zinke 5/10/2016 12:02 PM

Deleted: ure

427 products and HadISST, yet shows significant correlations with HadSST3, HadMAT1 and
428 HadNMAT2 (Suppl. Tabs. 11, 15, 16). Discrepancies between AT and gridded SST
429 products are observed between 1951 and 1955 with AT indicating significantly warmer
430 temperatures. Cabri tracks grid-SST between 1951 and 1955 while Totor shows warm
431 anomalies similar to AT. Taking into account the uncertainty of $\pm 0.33^{\circ}\text{C}$ based on the
432 regression error, however, Cabri SST agrees with gridded SST and AT within 1σ while
433 Totor shows less agreement.

434 For the period 1951 to 2005, we used AT, ERSSTv3b, ERSST4, HadISST,
435 HadSST3, HadMAT1 and HadNMAT2 to validate trends in annual mean coral Sr/Ca-
436 SST anomalies (Fig. 5). The uncertainty for the trend estimates in coral Sr/Ca SST is
437 calculated from the square root of the sum of squares of the regression error and the error
438 in the slope of the Sr/Ca-SST relationship. The long-term trends in Sr/Ca-derived SST
439 anomalies for the period 1951 to 2005 for Cabri and Totor converted to SST, using the
440 published Sr/Ca-SST relationship of -0.0607mmol/mol per 1°C , indicate a warming of
441 $1.38 \pm 0.39^{\circ}\text{C}$ and cooling of $-0.49 \pm 0.41^{\circ}\text{C}$, respectively. Instrumental SST indicate a
442 warming trend of $0.61 \pm 0.13^{\circ}\text{C}$ for HadISST, $0.72 \pm 0.11^{\circ}\text{C}$ for ERSST3b ($0.86 \pm 0.12^{\circ}\text{C}$
443 for ERSST4) and $0.78 \pm 0.12^{\circ}\text{C}$ for HadSST3. Air Temperature at Rodrigues weather
444 station recorded a warming trend of $0.46 \pm 0.17^{\circ}\text{C}$. All trends are statistically significant
445 at the 98% level with the exception of the negative trend in Sr/Ca SST anomalies in the
446 Totor core which is not significant.

447 For the pre-1945 period we used ERSSTv3b, HadISST, HadSST3 HadMAT1 and
448 HadNMAT2 to validate annual mean coral Sr/Ca-SST from core Totor (Fig. 2). We stress
449 that the number of SST observations in the ICOADS SST and marine AT database is

Jens Zinke 4/10/2016 4:22 PM

Deleted: 1

450 extremely sparse for our region (Fig. A3). In general, the Totor SST record is a valid
451 reconstruction for the region surrounding Rodrigues Island for several decades with the
452 possible exception of 1854-1860, 1916-1921, 1936-1941 and 1948-1951 (Fig. 2). The
453 Totor coral SST time series displays significantly higher SST anomalies compared to all
454 gridded SST reconstructions in the 1850's, between 1916-1921, 1936-1941 and 1948-
455 1951 and lower SST anomalies for brief periods between 1850 and 1890. Interestingly,
456 the Totor Sr/Ca-SST has significant correlations with HadSST3, HadMAT1 and
457 HadNMAT2 observational time series only (Suppl. Tabs. 11, 15, 16). The cool bias in
458 coral derived SST between 1882 and 1887 (core section 7) is related to diagenetic
459 alterations, but none of the anomalously warm periods can be explained by diagenesis
460 (see next section). We assessed the orientation of corallites relative to the coral slab
461 surface to test for sampling artifacts that might have altered our Sr/Ca data which we
462 summarized in Tables 2 and 3, illustrate in Figure 2 and discuss in section 6.1. Most
463 anomalous warm periods show sub-optimal orientation of sampling path with corallites at
464 an angle to the slab surface (see 6.1).

465

466 5.5 Large scale teleconnections between 1945 and 2006

467 The large-scale teleconnections with SST are significant for the Cabri Sr/Ca-SST
468 time series starting in 1945 (Figs. 6 and 7), while core Totor has statistically insignificant
469 correlations in that period. This indicates that the Cabri time series is more reliable for the
470 recent 60 years for monthly averages and annual means and shows the strongest
471 correlations across the Indo-Pacific (Figs. 6 and 7). Therefore, we assess the large-scale
472 climate teleconnections only for the period between 1945 and 2006.

Jens Zinke 4/10/2016 3:47 PM

Deleted: 7

Jens Zinke 4/10/2016 3:48 PM

Deleted: 8

Jens Zinke 4/10/2016 3:48 PM

Deleted: 7

Jens Zinke 4/10/2016 3:48 PM

Deleted: 8

478 The detrended Cabri Sr/Ca-SST records shows significant positive correlations for
479 austral summer and annual means with Indian Ocean wide SST, a positive significant
480 correlation with the central and eastern Pacific SST and negative significant correlations
481 with North Pacific SST typical for the spatial ENSO and PDO pattern (Figure 6;
482 Supplementary Tables 17-19). The detrended mean annual time scales (July-June) and
483 austral summer (JFM) record for the Cabri SST indicates a positive significant correlation
484 with southern Indian Ocean SST along a southeast to northwest band stretching along the
485 trade wind belt (Figure 6d-f). The correlation with the southern Indian Ocean trade wind
486 belt remains stable over different record length and is most pronounced post 1971. The
487 detrended Cabri record shows negative significant correlations ($r = -0.39$; $p < 0.001$; $N = 48$)
488 with the SIOD index for austral summer month. This agrees with similar sign and
489 strength of correlations of HadISST for Rodrigues with the SIOD ($r = -0.43$; $p < 0.001$;
490 $N = 48$; Fig. 1a; Tab. S19-21). We find positive significant correlations with the eastern
491 Pacific SST and negative correlations with the northern Pacific along 40°N and stretching
492 between 160°E and 150°W . The SST pattern mimics part of the typical spatial ENSO and
493 PDO pattern across the Indo-Pacific (Mantua et al., 1997; McPhaden et al., 2006).
494 Stratifying the correlations into negative and positive PDO phases between 1950-1975
495 and 1976 to 1999 reveals the PDO-like spatial SST pattern (Fig. 7).

496 Comparison with available coral proxy records from the wider trade wind belt
497 region in the SWIO between 12 to 21°S and 50 to 63°E reveals that the Cabri record
498 agrees best with the Sr/Ca-SST from St. Marie Island (core STM2 in Grove et al., 2013a;
499 $r = 0.25$; $N = 50$, $p = 0.08$; Fig. 8) on mean annual time scales, yet not with the La Reunion
500 record (not shown). Cabri shows the highest significant correlation of the three coral

Jens Zinke 4/10/2016 3:48 PM

Deleted: 7

Jens Zinke 4/10/2016 3:48 PM

Deleted: 7

Jens Zinke 5/10/2016 12:03 PM

Deleted: A3

Jens Zinke 4/10/2016 3:48 PM

Deleted: 8

Jens Zinke 4/10/2016 3:54 PM

Deleted: (Fig. 9)

506 records from SWIO with HadISST for the larger grid-box between 12 to 21°S and 50 to
507 63°E ($r=0.49$, $p=0.001$, $N=60$) while both St. Marie and La Reunion corals show no
508 statistically significant correlations.

509

510 **6 Discussion**

511 **6.1 Diagenesis, coral growth pattern changes and potential biases in Sr/Ca derived 512 SST**

513 Generally diagenesis could be excluded as a major cause of discrepancies between
514 coral SST and grid-SST. For core Totor, only for the period between 1882 and 1887 is
515 diagenesis the cause of a cool bias on our coral SST reconstruction (Figure 3d). Core
516 Cabri showed only localized positive Sr/Ca anomalies (cool SST bias) caused by
517 aragonitic sediment trapped within growth framework pores (Fig. 3f). These specific
518 samples have been removed before interpolation. Having excluded diagenesis for almost
519 all of the record, we assessed sampling biases due to changes in the orientation of growth
520 axes and positioning of corallites to the slab surface (Tab. 2 [and](#) 3). De Long et al. (2012)
521 showed clear evidence for warm or cool biases in coral Sr/Ca-SST reconstructions caused
522 by suboptimal orientation of corallites in corals from New Caledonia. We have adopted a
523 similar approach to test for sampling biases in our two cores (summarized in Table 2 [and](#)
524 3). We found that core Totor contained areas where a sampling bias could explain
525 anomalous Sr/Ca-derived SST (1781-1797, 1825-1835, 1854-1860, 1916-1921, 1936-
526 1941 and 1948-1951, 1984-2001). We provide a detailed explanation of the potential
527 biases in core Totor and its co-variability with a tropical western Indian Ocean coral SST

Jens Zinke 4/10/2016 4:24 PM
Deleted: &

Jens Zinke 4/10/2016 4:24 PM
Deleted: &

530 reconstruction from the Seychelles pre-1900 (Pfeiffer and Dullo, 2006; Fig. S2) in the
531 Supplementary Information that is of particular importance for coral paleoclimatologists.

532 De Long et al. (2012) showed that warm biases were often caused by corallites
533 orientated at an angle to the slab surface and where growth orientation had changed.
534 Sampling of these suboptimal intervals will have seasonal cycles with more summer
535 Sr/Ca values than winter values causing an apparent warm bias. Such a relationship could
536 not be identified for core Totor, for instance for the largest single warm anomaly in the
537 years 1916 to 1921. Nevertheless, the extreme warm anomaly between 1916 to 1921
538 could be associated with an unidentified vital effect (Alpert et al., 2015). Interestingly,
539 despite the potential influence of vital effects on the trend, the seasonality in this core
540 section was well preserved. This implies that seasonality can be captured robustly while
541 absolute values and trends are potentially biased by vital effects. This adds confidence for
542 the study of seasonality from fossil corals where vital effects are harder to distinguish
543 from true variability due to the lack of SST data for verification.

544 For the core tops between 1984 and 2005, Sr/Ca trends in cores Totor and Cabri
545 deviate with Totor showing a statistically insignificant cooling trend while Cabri shows a
546 strong warming trend (Fig. 2). Our analysis of polyp growth revealed a change in growth
547 pattern near the top of core Totor: the corallites form parallel, elongated rods of septa for
548 the entire period 1984 to 2005 (Fig. 9). Cabri shows a normal growth pattern, with an
549 optimal orientation of corallites at the core top between 1984 and 2006 (Fig. A5), with
550 the exception of sub-optimal corallites in the period 2000 to 2006. The core top of the
551 Totor coral skeleton has very low overall density compared to the pre-1984 record. The
552 Sr/Ca ratios show an increased seasonality, with colder winter values compared to core

Jens Zinke 4/10/2016 3:49 PM

Deleted: 6

554 Cabri, while summer values are not affected. At first glance, the peculiar structure of the
555 corallites in Totor would suggest optimal vertical growth of the corallites with the polyps
556 clearly visible from the apex of the core slab. This structure is, however, clearly
557 associated with high Sr/Ca ratios and artificially cold SST anomalies. A similar growth
558 pattern was found in a *Porites lutea* from St. Marie Island off East Madagascar (core
559 STM4 in Grove et al. 2013a). Grove et al. (2013a) ascribed the Sr/Ca trend difference
560 between cores STM2 and STM4 to changes in coral growth and calcification, yet their
561 results were not conclusive. Re-examination of core STM4 revealed that it also forms the
562 parallel-elongated rods of septa in the core top, which was biased towards high Sr/Ca
563 ratios and therefore cold SST anomalies. STM4 also showed low densities in this core top
564 section that agrees with low density in Totor. Inspection of various core sections in Totor
565 and other coral cores revealed that similar elongated rods of septa (not sampled down
566 core) are formed between neighboring growth fans of septa. We propose that these
567 parallel septa grow very fast in summer and winter, therefore show weak density contrast
568 with overall low skeletal density. Similar anomalously high Sr/Ca values between
569 adjacent fans of corallites were reported for Great Barrier Reef corals (see Figure 4 in
570 Alibert and McCulloch, 1997). Alibert and McCulloch (1997) suggested that less optimal
571 growth conditions may results in smaller corallites and overall low skeletal density
572 affecting Sr/Ca ratios. We suggest that core tops from *Porites* sp. with similar parallel
573 septa should be avoided for sampling since it can cause a cold bias in Sr/Ca-based SST
574 reconstructions.

575 Overall, our test for sampling biases to a large extend confirms the findings of De
576 Long et al. (2012) and indicates that such analysis should accompany climate

577 reconstructions from coral cores. Our results suggest that new cores need to be obtained
578 from the Totor colony or other large *Porites* sp. in order to overcome the SST biases
579 identified in the current record. The Cabri coral (>3.5m in height) would be an ideal site
580 since it provided an excellent and largely un-biased record of SST for the period 1945 to
581 2006. The 1907 dead surface was present, however, in three long cores drilled from the
582 Cabri coral at different angles, which could undermine the SST reconstruction for a few
583 decades below the mortality event. The reason for the mortality event could not be
584 determined.

585

586 **6.2 Trends and large-scale climate teleconnections since 1945 from core Cabri**

587 Based on our analysis of corallite orientations and diagenesis, we conclude that
588 core Cabri provides a largely un-biased record to assess SST trends and interannual
589 variability since 1945. The Cabri time series recorded a higher SST rise ($1.38 \pm 0.41^\circ\text{C}$)
590 than instrumental data between 1945 and 2006, which ranged between 0.61 to
591 $0.86 \pm 0.15^\circ\text{C}$. The trend in Cabri agrees with all SST datasets within 2σ , whereby the
592 lower range of uncertainty for the Cabri trend estimates ($\sim 1^\circ\text{C}$) is in close agreements to
593 trends from gridded SST datasets. Most of the accelerated warming trend in Cabri
594 resulted from the recent 6 years where the orientation of the corallites was sub-optimal.
595 We conclude that the SST trend in Cabri closely follows open ocean grid-SST which both
596 indicate strong warming ($\sim 0.68-1^\circ\text{C}$) of the south-central Indian Ocean over the past 60
597 years. Roxy et al. (2014) reported that during 1901–2012, the Indian Ocean warm pool
598 warmed by 0.78°C while the western Indian Ocean ($5^\circ\text{S}-10^\circ\text{N}$, $50^\circ-65^\circ\text{E}$) experienced
599 anomalous warming of 1.28°C in summer SSTs. Our results for Cabri are therefore not

Jens Zinke 4/10/2016 3:58 PM

Deleted: a

Jens Zinke 4/10/2016 3:58 PM

Deleted: s

602 unusual and within the range of observed Indian Ocean SST trends (Annamalei et al.,
603 2005; Alory et al., 2007; Koll Roxy et al., 2014). The strong warming in the southern
604 Indian Ocean trade wind belt could potentially alter the monsoon circulation, especially
605 during the monsoon onset phase in austral autumn (March to May; Annamalei et al.,
606 2005). Both, our Cabri coral SST time series and SST products indicate the strongest
607 warming for the March to May season (not shown). Rodrigues station precipitation is
608 strongly positively correlated with SST between March and May. When precipitation is
609 anchored over a warmer SWIO between March and May it can prevent the movements of
610 the ITCZ towards the North and potentially disrupt the Asian monsoon onset (Annamalei
611 et al., 2005).

612 The Cabri record also indicated that Rodrigues Island has negative correlations
613 with the SIOD. Rodrigues Island is located at the westernmost edge of the northeastern
614 flank of the SIOD that stretches from the south-central western Indian Ocean to the coast
615 of Western Australia. There is no other coral reef between Rodrigues Island and the West
616 Australian coast that is able to track the SIOD. Rodrigues is therefore the only coral reef
617 at which SST variability tracks the SIOD at its northeastern flank. The Ifaty corals off
618 southwest Madagascar was shown to track the southwestern flank of the SIOD (Zinke et
619 al., 2004). Our results suggest that a combination of corals off southwest Madagascar
620 with longer records from Rodrigues could provide valuable records of past SIOD
621 variability.

622 The Cabri coral SST reconstructions revealed a clear ENSO/PDO teleconnection
623 pattern for mean annual and austral summer averages with positive correlations across the
624 Indian Ocean in response to ENSO and PDO (Xie et al., 2016; Fig. 6 and 7; Suppl. Tabs.

Jens Zinke 4/10/2016 4:25 PM
Deleted: 7
Jens Zinke 4/10/2016 4:25 PM
Deleted: 8

627 17-19). The ENSO/PDO teleconnection was stable for the recent 60 years, yet appears
628 strongest between 1971 and 2006 (Fig. 6c,f). The latter period is known for increased
629 occurrence of El Niño events and a switch to a positive PDO phase up to 1999
630 (McPhaden et al., 2006). These results are in agreement with ENSO/PDO pattern
631 correlations observed in other coral records from the southwestern Indian Ocean (Pfeiffer
632 et al., 2004; Crüger et al., 2009). This is the first Indian Ocean coral SST reconstruction,
633 however, that shows a clear Indian Ocean SST relationship with the PDO. Previous
634 studies have shown only indirect links between the PDO with southwestern Indian Ocean
635 sea level pressure and salinity (Crueger et al., 2009), hydrological balance (Zinke et al.,
636 2008) and river runoff (Grove et al., 2013b). In addition, our record is the first Sr/Ca
637 record for the south-central Indian Ocean, which is currently the most reliable proxy for
638 SST in corals. The only long record from this region of the Indian Ocean is a stable
639 isotope record from La Reunion Island that mainly records salinity variations (Pfeiffer et
640 al., 2004). The lack of correlation between the La Reunion and Cabri record is therefore
641 not surprising and points to the need to develop Sr/Ca time series for La Reunion. The St.
642 Marie Island Sr/Ca coral record shows reasonable agreement with Cabri, with the SST
643 shift in the 1970's especially apparent in both records (Fig. 8). The St. Marie Island
644 record is, however, not well suited to track the wider trade wind belt variations.
645 Therefore, our new proxy record from Rodrigues for the period between 1945 and 2006 is
646 a valuable addition to the sparse Indian Ocean coral proxy network. It also establishes
647 that records from Rodrigues are well suited to study decadal climate teleconnections with
648 the (extra)tropical Pacific and the wider Indian Ocean.

649

Jens Zinke 4/10/2016 4:25 PM

Deleted: 7

Jens Zinke 4/10/2016 4:25 PM

Deleted: (Fig. 9)

Jens Zinke 4/10/2016 4:25 PM

Deleted: .

Jens Zinke 4/10/2016 4:26 PM

Deleted: 9

654 **7 Acknowledgements**

655 The coral paleoclimate work was supported as part of the SINDOCOM grant
656 under the Dutch NWO program ‘Climate Variability’, grant 854.00034/035. Additional
657 support comes from the NWO ALW project CLIMATCH, grant 820.01.009, and the
658 Western Indian Ocean Marine Science Association through the Marine Science for
659 Management program under grant MASMA/CC/2010/02. We thank the team of
660 SHOALS Rodrigues for their excellent support in fieldwork logistics and in the
661 organization of the research and CITES permits. We would also like to thank the
662 Rodrigues Assembly and the Mauritius Ministry for Fisheries for granting the research
663 and CITES permits. A Senior Curtin Fellowship in Western Australia, and an Honorary
664 Fellowship with the University of the Witwatersrand, South Africa, supported JZ. Bouke
665 Lacet and Wynanda Koot (VUA) helped cut the core slabs and prepared the thin sections.
666 Janice Lough and Eric Matson (AIMS) provided skilled technical support for coral core
667 densitometry measurements and data processing. We thank Dieter Garbe-Schönberg for
668 assistance with the ICP-OES measurements.

669

670 **References**

671 Alibert, C. and McCulloch M. T.: Strontium/calcium ratios in modern *Porites* corals from the
672 Great Barrier Reef as a proxy for sea surface temperature: calibration of the thermometer and
673 monitoring of ENSO, *Paleoceanography*, 12(3), 345-363, 1997.

674

675 Alory, G. and Meyers, G.: Warming of the Upper Equatorial Indian Ocean and Changes in the
676 Heat Budget (1960–99), *J. Climate*, 22, 93–113, 2009.

677

678 Alpert, A. E., Cohen, A. L., Oppo, D. W., DeCarlo, T. M., Gove, J. M., Young, C. W.
679 Comparison of equatorial Pacific sea surface temperature variability and trends with Sr/Ca

680 records from multiple corals. *Paleoceanography*, 31, 252-262, 2016.

681 Annamalai, H., Liu, P. and Xie, S.-P.: Southwest Indian Ocean SST Variability: Its Local
682 Effect and Remote Influence on Asian Monsoons, *Journal of Climate*, 18, 4150-4167, 2005.

683 Behera, S.K. and Yamagata, T. Subtropical SST dipole events in the southern Indian
684 Ocean, *Geophys. Res. Lett.* 28 (2), 327– 330, 2001.

685

686 Behera SK, Yamagata T. A dipole mode in the tropical Indian Ocean. *Geophysical Research*
687 *Letters*, 28, 327–330, 2001.

688

689 Carricart-Ganivet, J. P. and Barnes D. J.: Densitometry from digitized images of X-
690 radiographs: methodology for measurement of coral skeletal density, *Journal of Experimental*
691 *Marine Biology and Ecology*, 344, 67-72, 2007.

692

693 Charles, C. D., Hunter, D. E. and Fairbanks R. G.: Interaction between the ENSO and the Asian
694 Monsoon in a coral record of tropical climate, *Science*, 277, 925-928, 1997.

695

696 Cobb, K. M., Charles, C. D. and Hunter D. E.: A central tropical pacific coral demonstrates
697 pacific, Indian, and Atlantic decadal climate connections, *Geophysical Research Letters* 28(11),
698 2209-2212, 2001.

699

700 Cole, J. E., Dunbar, R. B., McClanahan, T. R. and Muthiga N. A.: Tropical Pacific forcing of
701 decadal SST variability in the Western Indian Ocean over the past two centuries. *Science* 287,
702 617-619, 2000.

703

704 Corrège, T., Sea surface temperature and salinity reconstruction from coral geochemical
705 tracers. *Palaeogeo. Palaeoclim. Palaeoeco.*, 232, 408-428, 2006.

706

707 Crueger, T., Zinke, J. and Pfeiffer M.: Patterns of Pacific decadal variability recorded by Indian
708 Ocean corals. *International Journal of Earth Sciences* 98, doi:10.007/s00531-00008-00324-
709 00531, 2009.

710

711 Deser, C., Phillips, A. S., and Hurrell, J. W.: Pacific Interdecadal climate variability:
712 linkages between the tropics and the North Pacific during boreal winter since 1900, *J.*
713 *Climate*, 17, 3109-3124, 2004.

714

715 DeLong, K. L., Quinn, T. M., Taylor, F. W., Shen, C.-C. and Lin, K.: Improving coral-base
716 paleoclimate reconstructions by replicating 350 years of coral Sr/Ca variations,
717 *Palaeogeography, Palaeoclimatology, Palaeoecology*, 373, 6-24, 2012.

718

719 DeVilliers, S., Sheng, G.T., Nelson, B.K.: The Sr /Ca-temperature relationship in coralline
720 aragonite: Influence of variability in (Sr/Ca)seawater and skeletal growth parameters,
721 *Geochimica et Cosmochimica Acta*, 58, 197-208, 1994.

722

723 Felis, T. and Paetzold, J.: Climate records from corals, In: *Marine Science Frontiers for*
724 *Europe*. Eds.: G. Wefer, F. Lamy and F. Mantoura. Berlin, Heidelberg, New York, Tokyo,
725 Springer, p. 11-27, 2003.

726

727 Funk, C., Dettinger, M. D., Michaelsen, J. C., Verdin, J. P., Brown, M. E., Barlow, M. and
728 Hoell, A.: Warming of the Indian Ocean threatens eastern and southern African food security
729 but could be mitigated by agricultural development, *Proceedings Nat. Acad. Sci.*, 105(32),
730 11081-11086, 2008.

731

732 Gagan, M. K., Dunbar, G. B. and Suzuki, A.: The effect of skeletal mass accumulation in
733 *Porites* on coral Sr/Ca and d18O paleothermometry, *Paleoceanography* 27, PA1203,
734 doi:10.1029/2011PA002215, 2012.

735

736

737 Grove, C. A., Kasper, S., Zinke, J., Pfeiffer, M., Garbe-Schönberg, D. and Brummer, G.-J. A.:
738 Confounding effects of coral growth and high SST variability on skeletal Sr/Ca: Implications
739 for coral paleothermometry, *Geochem., Geophys. Geosyst.*, 14, doi:10.1002/ggge.20095,
740 2013a.

741

742 Grove, C. A., Zinke, J., Peeters, F., Park, W., Scheufens, T., Kasper, S.,
743 Randriamanantsoa, B., McCulloch, M. T. and Brummer, G.J.A. Madagascar corals reveal
744 multidecadal modulation of rainfall since 1708. *Climate of the Past* 9, 641-656, 2013b.
745

746 Hardman, E. R., Meunier, M. S., Turner, J. R., Lynch, T. L., Taylor, M. and Klaus R.: The
747 extent of coral bleaching in Rodrigues, *Journal of Natural History*, 38, 3077-3089, 2004.
748

749 Hardman, E. R., Stampfli, N. S., Hunt, L., Perrine, S., Perry, A. and Raffin, J. S.: The Impacts
750 of coral bleaching in Rodrigues, Western Indian Ocean, *Atoll Research Bulletin*, 555, DOI:
751 10.5479/si.00775630.555.1, 2008.
752

753 Helmle, K. P., Dodge, R.E., Swart, P.K., Gledhill, D.K. and Eakin, C.M.: Growth rates of
754 Florida corals from 1937 to 1996 and their response to climate change, *Nat. Commun.* 2, 215
755 doi: 10.1038/ncomms1222, 2011.
756

757 Hendy, E. J., Gagan, M. K., Lough, J. M., McCulloch, M., and deMenocal P. B.: Impact of
758 skeletal dissolution and secondary aragonite on trace element and isotopic climate proxies in
759 Porites corals, *Paleoceanography*, 22, PA4101, doi:10.1029/2007PA001462, 2007.
760

761 Hoell, A., Funk, C., Zinke, J., Harrison, L. Modulation of the Southern Africa precipitation
762 response to the El Niño Southern Oscillation by the subtropical Indian Ocean Dipole. *Climate
763 Dynamics*, DOI:10.1007/s00382-00016-03220-00386, 2016.
764

765 Jones, P. The Reliability of Global and Hemispheric Surface Temperature Records. *Advances in
766 Atmospheric Sciences*, 33, 269-282, 2016.
767

768 Kaplan, A., Cane, M. A., Kushnir, Y., Clement, A. C., Blumenthal, M. B., Rajagopalan, B.
769 Analyses of global sea surface temperature 1856-1991, J. Geophys. Res., 103, 18567-18589,
770 1998.

771

772 Kennedy J.J., Rayner, N.A., Smith, R.O., Saunby, M. and Parker, D.E.: Reassessing biases and

Jens Zinke 5/10/2016 10:36 AM
Deleted: *et al.*

774 other uncertainties in sea-surface temperature observations since 1850 part 1: measurement and
775 sampling errors, *J. Geophys. Res.*, 116, D14103, doi:10.1029/2010JD015218, 2011.

776

777 Kent, E.C., Rayner N.A., Berry D.I., Saunby M., Moat B.I., Kennedy J.J., Parker D.E.: Global
778 analysis of night marine air temperature and its uncertainty since 1880: the HadNMAT2
779 Dataset, *Journal of Geophys. Res.*, doi: 10.1002/jgrd.50152, 2013.

780

781 Koll Roxy, M., Ritika, K., Terray, P., Masson, S.: The curious case of Indian Ocean warming,
782 *Journal of Climate* 27, 8501-8509, 2014.

783

784 Krishnan, P., and Sugi, M.: Pacific decadal Oscillation and variability of the Indian
785 summer monsoon rainfall, *Climate Dynamics*, 21, 233-242, 2003.

786

787 Lee, S.-K., Park, W., Baringer, M. O., Gordon, A. L., Huber, B. and Liu ,Y.: Pacific origin of
788 the abrupt increase in Indian Ocean heat content during the warming hiatus, *Nature Geoscience*,
789 8, 445-449, 2015.

790

791 Lynch T.L., Meunier, M.S., Hooper, T.E.J., Blais, F.E.I., Raffin, J.S.J, Perrine, S., Félicité, N.,
792 Lisette, J., Grandcourt, J.W.: Annual report of benthos, reef fish and invertebrate surveys for
793 Rodrigues 2002, Shoals Rodrigues report, 30pp, 2002.

794

795 Mantua, N. J., Hare, S. R., Zhang, Y., Wallace, J. M., and Francis, R. C.: A Pacific decadal
796 climate oscillation with impacts on salmon, *Bull. Amer. Meteor. Soc.*, 78, 1069–1079, 1997.

797

798 Mart, Y.: The tectonic setting of the Seychelles, Mascarene and Amirante plateaus in the
799 Western Equatorial Indian ocean, *Marine Geology*, 79, 261-274, 1988.

800

801 McGregor H. V. and Gagan M. K.: Diagenesis and geochemistry of Porites corals from Papua
802 New Guinea: implications for paleoclimate reconstruction, *Geochim. Cosmochim. Acta*, 67,
803 2147–2156, 2003.

804

805 McGregor, H. V. and Abram, N. J.: Images of diagenetic textures in Porites corals from Papua
806 New Guinea and Indonesia, *Geochemistry, Geophysics, Geosystems* 9(10),
807 doi:10.1029/2008GC002093, 2008.

808

809 McPhaden, M. J., Zebiak, S. E., Glantz, M. H.: ENSO as an Integrating Concept in Earth
810 Science, *Science*, 314, 1740-1745, 2006.

811

812 Meehl, G. A., and Hu, A.: Megadroughts in the Indian Monsoon Region and Southwest North
813 America and a mechanism for associated Multidecadal Pacific Sea Surface Temperature
814 Anomalies, *J. Climate*, 19, 1605-1623, 2006.

815

816 Nakamura, N., Kayanne, H., Iijima, H., McClanahan, T. R., Behera, S. K. and Yamagata, T.:
817 Mode shift in the Indian Ocean climate under global warming stress, *Geophysical Research
818 Letters*, 36, L23708, doi:10.1029/2009GL040590, 2009.

819

820 New A. L., Alderson S. G., Smeed D.A., Stansfield K.L.: On the circulation of water masses
821 across the Mascarene Plateau in the South Indian Ocean, *Deep-Sea Research I* 54, 42–74, 2007.

822

823 New A. L., Stansfield, K., Smythe-Wright, D., Smeed D. A., Evans, A. J. and Alderson, S. G.:
824 Physical and biochemical aspects of the flow across the, Mascarene Plateau in the Indian
825 Ocean, *Philosophical Transactions of the Royal Academic Society* 363, 151–168, 2005.

826

827 Nurhati, I. S., Cobb, K. M. and Lorenzo E. D. Decadal-Scale SST and Salinity Variations in the
828 Central Tropical Pacific: Signatures of Natural and Anthropogenic Climate Change. *Journal of
829 Climate* 24: 3294-3308, 2011.

830

831 Paillard, D., Labeyrie, L., Yiou, P.: Macintosh program performs time series analysis. *Eos
832 Trans AGU* 77, 379, 1996.

833

834 Pfeiffer, M., Timm, O. and Dullo, W.-C.: Oceanic forcing of interannual and multidecadal
835 climate variability in the southwestern Indian Ocean: Evidence from a 160 year coral isotopic
836 record (La Reunion, 50E, 21S). *Paleoceanography*, 19, PA4006, doi:10.1029/2003PA000964,
837 2004.

838

839 Pfeiffer M. and Dullo, W.-Ch. Monsoon-induced cooling of the western equatorial Indian
840 Ocean as recorded in coral oxygen isotopes records from the Seychelles covering the period
841 1840-1994 AD. *Quat Sci Rev* 25:993–1009, 2006.

842

843 Pfeiffer, M., Dullo, W.-C., Zinke, J. and Garbe-Schoenberg, D.: Three monthly coral Sr/Ca
844 records from the Chagos Archipelago covering the period of 1950-1995 A.D.: reproducibility
845 and implications for quantitative reconstructions of sea surface temperature variations,
846 *International Journal of Earth Sciences*, 98, doi:10.1007/s00531-00008-00326-z, 2009.

847

848 Rayner, N. A., Parker, D. E., Horton, E. B., Folland, C. K., Alexander, L. V., Rowell, D. P.,
849 Kent, E. C. and Kaplan A.: Global analyses of sea surface temperature, sea ice, and night
850 marine air temperature since the late nineteenth century. *Journal of Geophysical Research*
851 108(D14), doi:10.1029/2002JD002670, 2003.

852

853 Reason, C.J.C. Subtropical Indian Ocean SST dipole events and southern African rainfall,
854 *Geophys. Res. Lett.*, 28 (11) 2225–2227, 2001.

855

856 Reynolds, R.W., Rayner, N.A., Smith, T.M., Stokes, D.C., Wang W.: An improved in situ and
857 satellite SST analysis for climate, *Journal of Climate*, 15, 1609–1625, 2002.

858

859 Reynolds, R. W., Smith, T. M., Liu, C., Chelton, D. B., Casey, K. S. and Schlax, M. G.: Daily
860 high-resolution blended analyses for sea surface temperature, *J. of Climate*, 20, 5473-5496,
861 2007.

862

863 Sayani, H. R., Cobb, K. M., Cohen, A. L., Crawford Elliott, W., Nurhati, I. S., Dunbar, R. B.,
864 Rose, K. A., Zaunbrecher, L. K.: Effects of diagenesis on paleoclimate reconstructions from
865 modern and young fossil corals, *Geochimica et Cosmochimica Acta*, 75, 6361–6373, 2011.

866

867 Schott, F.A., McCreary, J.P.: The monsoon circulation of the Indian Ocean, *Progress in*
868 *Oceanography*, 51, 1–123, 2001.

869

870 Schrag, D.P.: Rapid analyses of high-precision Sr/Ca ratios in corals and other marine
871 carbonates, *Paleoceanography*, 14, 2, 97-102, 1999.

872

873 Sheppard, C.R.C. Predicted recurrences of mass coral mortality in the Indian Ocean.
874 *Nature*, 425, 294-297, 2003.

875

876 Smith, T.M., Reynolds, R.W., Peterson, T.C., Lawrimore, J.: Improvements to NOAA's
877 historical merged land–ocean surface temperature analysis (1880–2006), *J. of Climate*, 21,
878 2283, 2008.

879

880 Smodej, J., Reuning, L., Wollenberg, U., Zinke, J., Pfeiffer, M. and Kukla, P. A.: Two-
881 dimensional X-ray diffraction as a tool for the rapid, nondestructive detection of low calcite
882 quantities in aragonitic corals, *Geochemistry, Geophysics, Geosystems*, 16,
883 10.1002/2015GC006009, 2015.

884

885 Tokinaga, H., Xie, S.P., Deser, C., Kosaka, Y., Okumura, Y. M.: Slowdown of the
886 Walker circulation driven by tropical Indo-Pacific warming. *Nature*, 491, 439-444, 2012.

887

888 [Trouet, V. and van Oldenborgh, G.J. KNMI Climate Explorer: a web-based research tool for high-resolution paleoclimatology. *Tree Ring Research*, 69, 1, 3-13 \(2013\).](#)

889

890

891 Turner, J. and Klaus, R.: Coral reefs of the Mascarenes, Western Indian Ocean, *Philosophical*
892 *transactions of the Royal Academic Society*, 363, 229–250, 2005.

Jens Zinke 4/10/2016 3:23 PM
Formatted: Font:
Jens Zinke 4/10/2016 3:23 PM
Formatted: Normal, No bullets or numbering
Jens Zinke 4/10/2016 3:23 PM
Formatted: Font:
Jens Zinke 4/10/2016 3:23 PM
Formatted: Font:Not Italic
Jens Zinke 4/10/2016 3:23 PM
Formatted: Font:Not Bold
Jens Zinke 4/10/2016 3:23 PM
Deleted: .

894

895 van Oldenborgh, G. J., Burgers, G.: Searching for decadal variations in ENSO
896 precipitation teleconnections, *Geophys. Res. Lett.*, 32, L15701, 2005.

897

898 Woodruff, S.D. *et al.*: ICOADS Release 2.5: Extensions and enhancements to the surface
899 marine meteorological archive, *Int. J. Climatol.*, 31, 951-967, 2011.

900

901 Xie, S.-P., Kosaka Y., Du Y., Hu K. M., Chowdary J. S., and Huang G.: Indo-western Pacific
902 ocean capacitor and coherent climate anomalies in post-ENSO summer: A review, *Adv. Atmos.*
903 *Sci.*, 33(4), 411–432, 2016.

904

905 Zinke, J., Pfeiffer, M., Park, W., Schneider, B., Reuning, L., Dullo, W.-Chr., Camoin, G. F.,
906 Mangini, A., Schroeder-Ritzrau, A., Garbe-Schönberg, D. and Davies, G. R.: Seychelles coral
907 record of changes in sea surface temperature bimodality in the western Indian Ocean from the
908 Mid-Holocene to the present, *Climate Dynamics*, 43 (3), 689-708, 2014.

909

910 Zinke, J., Pfeiffer, M., Timm, O., Dullo, W.-Chr. and Brummer, G. J. A. Western Indian
911 Ocean marine and terrestrial records of climate variability: a review and new concepts on
912 land-ocean interaction since A.D. 1660. *International Journal of Earth Sciences* 98,
913 Special Volume. doi:10.1007/s00531-008-0365-5, 2009.

914

915 Zinke, J., Timm, O., Pfeiffer, M., Dullo, W.-Chr., Kroon, D. and Thomassin, B. A.
916 Mayotte coral reveals hydrological changes in the western Indian between 1865 to 1994.
917 *Geophysical Research Letters* 35, L23707, doi:10.1029/2008GL035634, 2008.

918

919 Zinke, J., Dullo, W.-Chr., Heiss, G. A. & Eisenhauer, A. ENSO and subtropical dipole
920 variability is recorded in a coral record off southwest Madagascar for the period 1659 to
921 1995. *Earth and Planetary Science Letters* 228 (1-2), 177-197, 2004.

922

923 **Tables**

Core name	GPS position	Species	Water depth (m)	Mean growth rate mm year ⁻¹	Mean density g/cm ³	Mean Calcification rate g/cm ² year ⁻¹
Totor	S19°40.237; E63°25.754	<i>Porites sp.</i>	4.0	9.2 (±0.19)	1.128 (±0.11)	1.07 (±0.18)
Cabri	S19°40.030, E63°26.065	<i>Porites lobata</i>	3.0	11.8 (±0.25)	1.36 (±0.12)	1.60 (±0.16)

924 Table 1 - Coral cores with their GPS co-ordinates and colony depths at low tide, with
 925 mean rates of extension, density, and calcification over the complete length of the
 926 individual records (1907 to 2006 for Cabri; 1781 to 2005 for Totor).

Jens Zinke 4/10/2016 3:59 PM

Deleted: ies

927

928

929

930

931

932

933

934

935

936

937

938

939

940

941

Section	Year	Orientation	Bias	Notes
1	2005-1987	Sub-optimal	cool	Corallites parallel to surface, yet straight angle; probably like a valley
2	1987-1982	Sub-optimal	cool	Corallites parallel to surface, yet straight angle; probably like a valley
2	1981-1977	Sub-optimal	none	Corallites at an angle to the surface; no bias
3	1978-1975	Sub-optimal	none	Corallites at an angle to the surface; no bias
3	1974-1958	Optimal	none	Corallites parallel to surface; no bias
4A	1958-1952	Sub-optimal	warm	Corallites at an angle to the surface; scallop texture from angles of corallites
4A	1951-1945	Sub-optimal	warm	Corallites at an angle to the surface; 1947-1952 low growth rate; reduced seasonality
4B	1947-1936	Optimal	none	Corallites parallel to surface, 1945-1947 better orientation than in slab 4A
4B	1938-1933	Sub-optimal	none	Corallites at an angle to the surface; 1936-1941 warm anomaly years show normal seasonality and high growth rate
5	1933-1922	Optimal	none	Corallites parallel to surface; 1922-1928 reduced seasonality
6	1921-1915	Sub-optimal	warm	1915-21 warm spikes shows slightly oblong corallites, yet normal seasonality; switch from optimal to sub-optimal orientation
6	1915-1896	Optimal to Sub-optimal	none	Corallites mostly parallel to surface, small section with corallites at slight angle;;
7	1897-1890	Optimal	none	Corallites parallel to surface
7	1887-1882	Optimal	cool	Diagenesis detected between years 1882-1887
7	1881-1872	Sub-optimal	none	Corallites at an angle to the surface; 1872 close to bioerosion track; 1878-1880 low seasonality, yet no effect
8	1872-1868	Sub-optimal	cool	Corallites at an angle to the surface; some corallites at almost 90° angle; 1868-1872 below bioerosion track; 1867-1871 low seasonality
9	1860-1854	Sub-optimal	warm	Corallites at an angle to the surface; 1854-1858 low seasonality, less winter samples
9	1856-1845	Sub-optimal	warm	Corallites parallel to surface; low seasonality with relatively warm winter samples
9	1844-1831	Optimal	none	Corallites parallel to surface; only 1831-1832 corallites at an angle to surface
10	1830-1827	Sub-optimal	warm	Corallites at an angle to the surface; oblong orientation
10	1826-1823	Disorganised	warm	Corallites rotating at 90° angle; low growth rate, seasonality reduced 1823-1825 with relatively warm winter samples
10	1822-1815	Optimal	none	Corallites parallel to surface; low growth rate; reduced seasonality 1818-1822, yet no effect on SST anomalies
11	1816-1806	Sub-optimal	none	Corallites at an angle to the surface, yet no effect on SST anomalies
11	1807-1798	Sub-optimal	none	Corallites at an angle to the surface in sub-optimal parts; Corallites rotating at 90° angle near terminating fans (not sampled); 3 growth axes with terminating fans in between (not sampled); 1799-1807 regular seasonality
11	1797-1792	Sub-optimal	warm	Corallites at an angle to the surface
12	1795-1792	Disorganised	warm	Corallites rotating at 90° angle; 1792-1791 long year, more summer samples
12	1791-1784	Sub-optimal	warm	Corallites parallel to surface; 1784-1787 Corallites at an angle to the surface; 1789-1794 seasonality distorted
12	1781-1783	Disorganised	warm	Corallites rotating at 90° angle; seasonality slightly distorted, apparently more summer samples

943 Table 2 – Summary of sampling issues detected in core Totor. Unbiased sampling tracks
 944 indicated in bold.

Section	Year	Orientation	Bias	Notes
1	2007-2000	Sub-optimal	warm	Corallites parallel to surface; yet no clear growth fans
1	1999-1992	Optimal	none	Corallites parallel to surface
2	1984-1992	Sub-optimal	none	Corallites at an angle to the surface; oblong corallites
3	1983-1968	Sub-optimal	none	Corallites parallel to surface; yet no clear growth fan
4	1967-1964	Sub-optimal	none	Corallites at an angle to the surface
5	1963-1958	Optimal	none	Corallites parallel to surface
5	1957-1954	Sub-optimal	none	Corallites at an angle to the surface
5	1953-1945	Optimal	none	Corallites parallel to surface

945

946 Table 3 – Summary of sampling issues detected in core Cabri. Unbiased sampling tracks
 947 indicated in bold.

948

949 **Figure captions**

950 Figure 1 – a) Map of Rodrigues Island with the position of the two corals cores at Totor
 951 and Cabri indicated. The star shows the position of the CTD that collects SST and salinity
 952 data. Polygon indicates the location of the Meteorological Station which records air
 953 temperature, sunshine hours, wind speed and rainfall. b) Spatial correlation between
 954 January-March averaged SIOD index (Behera and Yamagata, 2001) with HadISST for
 955 Rodrigues Island (Rayner et al., 2003). c) Spatial correlation between July-June mean
 956 annual averaged PDO index (Mantua et al., 1997) with HadISST (Rayner et al., 2003).
 957 All correlations with detrended data. Only correlation with $p < 0.05$ are coloured.
 958 Computed at KNMI climate explorer (van Oldenborgh and Burgers, 2005). Yellow star in
 959 b) and c) marks the location of Rodrigues Island.

960

961 Figure 2 – a) Time series of monthly (thin solid lines) Sr/Ca anomalies (right Y-axis
 962 converted) relative to the 1961 to 1990 climatological mean for coral cores Cabri (top),
 963 Totor (middle) for the period 1781 to 2006. Annual mean time series of individual cores
 964 (red line) b) Cabri and c) Totor compared to SST reconstructions: ERSSTv3b, ERSSTv4,
 965 HadISST, HadSST3, HadMAT1 and HadNMAT2. See legend in b) and c) for colour

966 code. For all time series we computed anomalies relative to 1961 to 1990. The
967 uncertainty of mean annual coral Sr/Ca-SST anomalies is indicated by the grey envelope.
968 Potential warm bias in coral SST is indicated in parathenses, pointing up for warm and
969 down for potential cool biases, respectively. Parathenses with inset D marks core interval
970 with diagenesis.

971

972 Figure 3 - Thin-section and SEM images of primary coral aragonite (PA) and aragonite
973 cement (AC) in cores Totor and Cabri. A and B: Excellent preservation of the primary
974 coral aragonite in core [section 4A and 4B in](#) Totor. Trace amounts of aragonite cements
975 occur as isolated patches in core sections 6 (C), 7 (D) and 11 (E) of Totor. F (left): A
976 prominent growth break (stippled line) in core section 12 of Totor is encrusted by
977 coralline red algae (CRA). F (middle): The section above the growth break shows well
978 preserved primary coral aragonite. F (right): The pristine coral skeleton of core Cabri
979 contains locally aragonitic sediment (S) partially filling growth-framework pores. A to E:
980 Thin section photographs are shown in plane- (left) and cross-polarized light (middle). F:
981 All thin section photographs are shown in plane-polarized light.

982

983 Figure 4 – a) Climatology at Rodrigues between 1997 to 2007. Monthly averaged SST *in*
984 *situ* (red), ERSSTv.3b (grey; Smith et al., 2008) and AVHRR SST (blue stippled;
985 Reynolds et al., 2007); b) Reconstructed absolute SST from coral Sr/Ca from cores Totor
986 (dark grey with triangle) and Cabri (light grey with diamond) for 2002 to 2006 based on
987 calibration with *in situ* SST from Rodrigues (red). The uncertainty for single month

988 absolute SST for individual cores Cabri and Totor is 1.23°C and 1.05°C (1 σ),
989 respectively. The coral data agree with *in situ* SST within the 1 σ uncertainty.

990

991 Figure 5 – Time series of annual mean temperatures anomalies relative to the 1961-1990
992 mean for the coral Cabri SST reconstruction, Rodrigues weather station air temperature
993 (AT), ERSSTv3b, ERSSTv4, HadISST, HadSST3, HadMAT1 and HadNMAT2 for the
994 period 1950 to 2006. The uncertainty of mean annual coral Sr/Ca-SST anomalies is
995 indicated by the grey envelope.

996

997 Figure 6 – Spatial correlation of Cabri Sr/Ca-SST anomalies (relative to 1961-1990) with
998 HadISST (Rayner et al., 2003). January to March austral summer in a) between 1945-
999 2006, b) 1961-1990 and c) 1971-2006. Annual mean correlations in d) between 1945-
1000 2006, e) 1961-1990 and f) 1971-2006. Only correlation with $p < 0.05$ is coloured.
1001 Computed at KNMI climate explorer (van Oldenborgh and Burgers, 2005). Yellow star in
1002 a) marks location of Rodrigues Island.

1003

1004 Figure 7 – Spatial correlations of Left) Cabri coral SST and Right) HadISST grid for
1005 Rodrigues Island with global austral summer HadISST for a-c) 1950 to 1975 (February to
1006 May) negative PDO phase (Mantua et al., 1997) and c-d) 1976 to 1999 (January to April)
1007 positive PDO phase. Only correlations with $p < 0.05$ coloured. Computed at KNMI climate
1008 explorer (van Oldenborgh and Burgers, 2005). Yellow star in a) marks location of
1009 Rodrigues Island.

1010

Jens Zinke 4/10/2016 4:26 PM

Deleted: 1

Jens Zinke 4/10/2016 4:26 PM

Deleted: Figure 6 – a) Monthly interpolated Sr/Ca profiles for cores Cabri (red) and Totor (grey). b) Images of core Totor (coloured blue) with orientation of corallites indicated. Years for core sections indicated on coral slab and grey arrow points to major change in growth pattern in Totor core top section around the years 1983/84.

Jens Zinke 4/10/2016 4:26 PM

Deleted: 7

Jens Zinke 4/10/2016 4:26 PM

Deleted: 8

1022 | Figure 8 – Comparison of Southwestern Indian Ocean (SWIO) coral records from St.
1023 | Marie Island (black; Grove et al., 2013) with the Cabri record from Rodrigues (red). A
1024 | SST time series for the grid-box in the SWIO averaged between 12-20°S and 50-63°E is
1025 | also illustrated (light blue). All time were annualized and converted to SST anomalies
1026 | relative to 1961-1990. The uncertainty of mean annual Cabri Sr/Ca-SST anomalies is
1027 | indicated by the grey envelope.

1028 |
1029 | Figure 9 – a) Monthly interpolated Sr/Ca profiles for cores Cabri (red) and Totor (grey).
1030 | b) Images of core Totor (coloured blue) with orientation of corallites indicated. Years for
1031 | core sections indicated on coral slab and grey arrow points to major change in growth
1032 | pattern in Totor core top section around the years 1983/84.

1033 |
1034 | Figure A1 – X-ray negative print for core sections of core Totor with sampling lines
1035 | indicated. Blue lines indicate high resolution sampling tracks. Yellow lines superimposed
1036 | on blue lines indicate sampling at annual resolution for other purposes. Start or end years
1037 | for each core section indicated.

1038 |
1039 | Figure A2 - X-ray negative print for core sections of core Cabri with sampling lines
1040 | (milling holes) indicated. Start or end years for each core section indicated. Note the dead
1041 | surface before 1907 that is most probably related to a past coral bleaching event.

1044 | Figure A3 – Number of SST observations in the grid box surrounding Rodrigues in the
1045 | ICOADS database. Note the extremely sparse observations even in recent years (van
1046 | Oldenborgh and Burgers, 2005).

Jens Zinke 4/10/2016 4:26 PM
Deleted: 1

1047

1048 | Figure A4 – Spatial correlations of mean annual HadMAT1 air temperature anomalies
1049 | between 1945 to 2001 relative to 1961-1990 with a) HadISST for Rodrigues, and b) Cabri
1050 | SST. Only correlations with $p < 0.05$ coloured. Computed at KNMI climate explorer (van
1051 | Oldenborgh and Burgers, 2005). Y-axis Latitude, X-axis Longitude.

Jens Zinke 5/10/2016 4:32 PM
Deleted: 2

1052 |

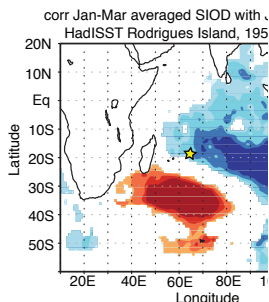
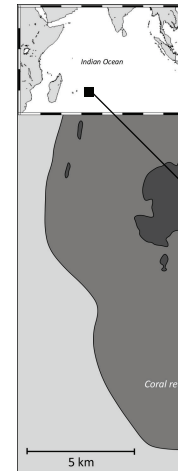
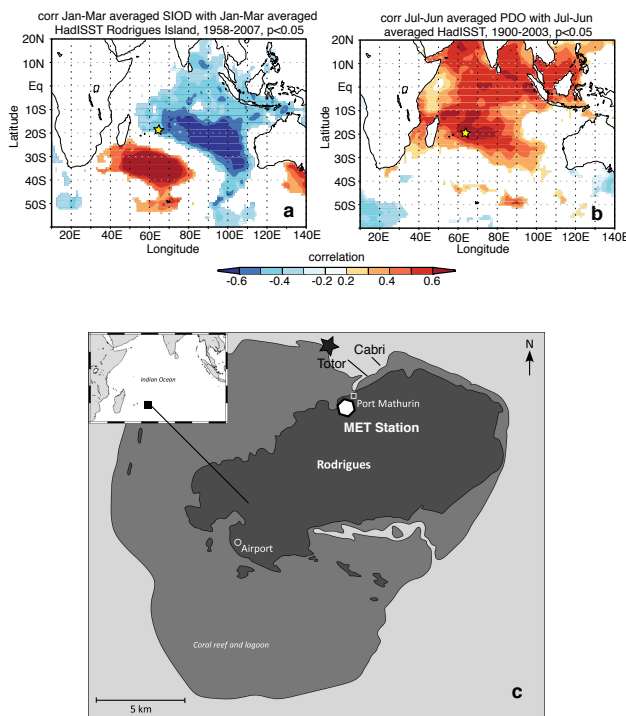
1053 | Table A1 – Statistics of various sea surface temperature (SST) products and air
1054 | temperature for Rodrigues with 1σ standard deviations in brackets for the period 2002 to
1055 | 2006 (period with *in situ* SST data). STDV = 1σ standard deviation over all years. All
1056 | units in °C.

Jens Zinke 5/10/2016 4:32 PM
Deleted: 1 ... [1]

1057

1058 | Table A2 - Linear regression of coral Sr/Ca with a) *in situ* SST 2002-2005/6, b)
1059 | ERSSTv.3 (Smith et al., 2008) 1997-2005/6, c) AVHRR SST NOAA Coral Reef watch
1060 | data 2000-2005/6 and d) monthly Sr/Ca with AVHRR SST (Reynolds et al., 2007) for the
1061 | period 1982 to 2005.

1062



Deleted:

Jens Zinke 4/10/2016 4:32 PM

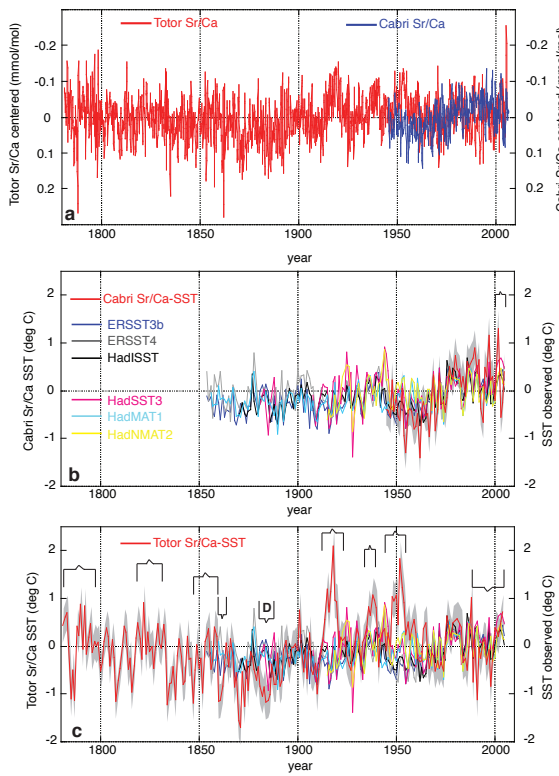
Moved down [1]:) Map of Rodrigues Island with the position of the two corals cores at Totor and Cabri indicated. The star shows the position of the CTD that collects SST and salinity data. Polygon indicates the location of the Meteorological Station which records air temperature, sunshine hours, wind speed and rainfall.

Deleted: a

Deleted: b

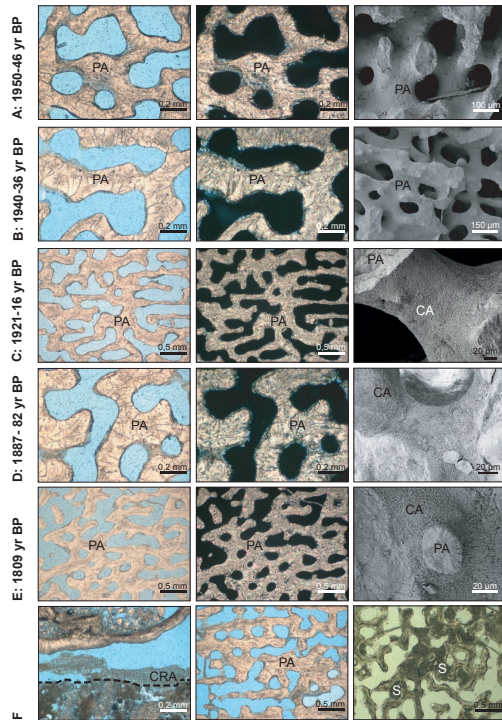
Deleted: c

1067
1068 Figure 1 – a) Spatial correlation between January-March averaged SIOD index (Behera
1069 and Yamagata, 2001) with HadISST (Rayner et al., 2003) for Rodrigues Island. b) Spatial
1070 correlation between July-June mean annual averaged PDO index (Mantua et al., 1997)
1071 with HadISST (Rayner et al., 2003). All correlations with detrended data. Only
1072 correlation with $p < 0.05$ are coloured. Computed at KNMI climate explorer (van
1073 Oldenborgh and Burgers, 2005). Yellow star in a) and b) marks the location of Rodrigues
1074 Island. c) Map of Rodrigues Island with the position of the two corals cores at Totor and
1075 Cabri indicated. The star shows the position of the CTD that collects SST and salinity
1076 data. Polygon indicates the location of the Meteorological Station which records air
1077 temperature, sunshine hours, wind speed and rainfall.



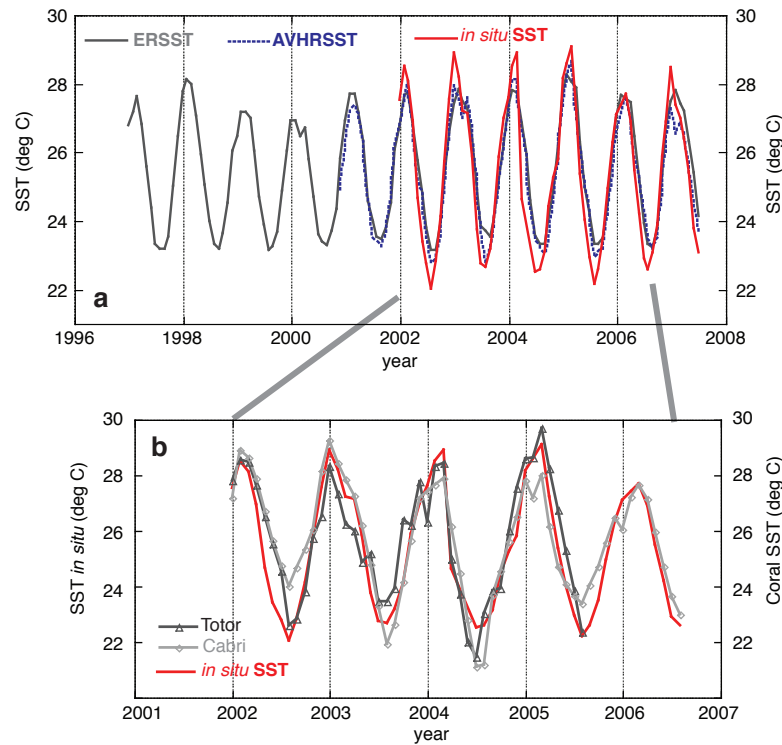
1098
1099 Figure 2 - a) Time series of monthly (thin solid lines) Sr/Ca anomalies (right Y-axis
1100 inverted) relative to the 1961 to 1990 climatological mean for coral cores Cabri (top),
1101 Totor (middle) for the period 1781 to 2006. Annual mean time series of individual cores
1102 (red line) b) Cabri and c) Totor compared to SST reconstructions: ERSSTv3b, ERSSTv4,
1103 HadISST, HadSST3, HadMAT1 and HadNMAT2. See legend in b) and c) for colour
1104 code. For all time series we computed anomalies relative to 1961 to 1990. The
1105 uncertainty of mean annual coral Sr/Ca-SST anomalies are indicated by the grey
1106 envelope. Potential warm bias in coral SST is indicated by brackets, pointing up for warm
1107 and down for potential cool biases, respectively. Bracket with inset D marks core interval
1108 with diagenesis.
1109

Jens Zinke 4/10/2016 4:00 PM
Deleted: co

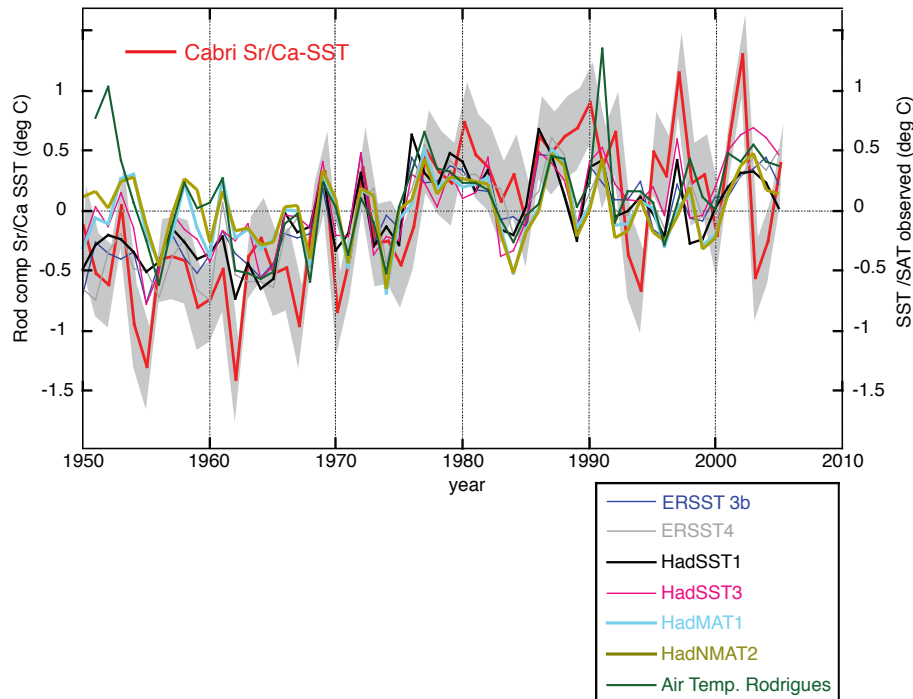


1111

1112 Figure 3 - Thin-section and SEM images of primary coral aragonite (PA) and aragonite
 1113 cement (AC) in cores Totor and Cabri. A and B: Excellent preservation of the primary
 1114 coral aragonite in core [sections 4A and 4B in](#) Totor. Trace amounts of aragonite cements
 1115 occur as isolated patches in core sections 6 (C), 7 (D) and 11 (E) of Totor. F (left): A
 1116 prominent growth break (stippled line) in core section 12 of Totor is encrusted by
 1117 coralline red algae (CRA). F (middle): The section above the growth break shows well
 1118 preserved primary coral aragonite. F (right): The pristine coral skeleton of core Cabri
 1119 contains locally aragonitic sediment (S) partially filling growth-framework pores. A to E:
 1120 Thin section photographs are shown in plane- (left) and cross-polarized light (middle). F:
 1121 All thin section photographs are shown in plane-polarized light.



1124 Figure 4 – a) Climatology at Rodrigues between 1997 to 2007. Monthly averaged SST
 1125 *in situ* (red), ERSSTv.3 (grey; Smith et al., 2008) and AVHRR SST (blue stippled;
 1126 Reynolds et al., 2007); b) Reconstructed absolute SST from coral Sr/Ca from cores Totor
 1127 (dark grey with triangle) and Cabri (light grey with diamond) for 2002 to 2006 based on
 1128 calibration with *in situ* SST from Rodrigues (red). The uncertainty for single month
 1129 absolute SST for individual cores Cabri and Totor is 1.23°C and 1.05°C (1σ),
 1130 respectively. The coral data agree with *in situ* SST within the 1σ uncertainty.



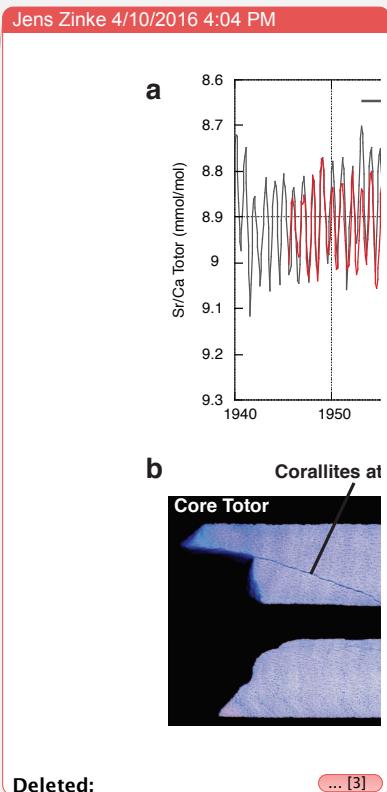
1132

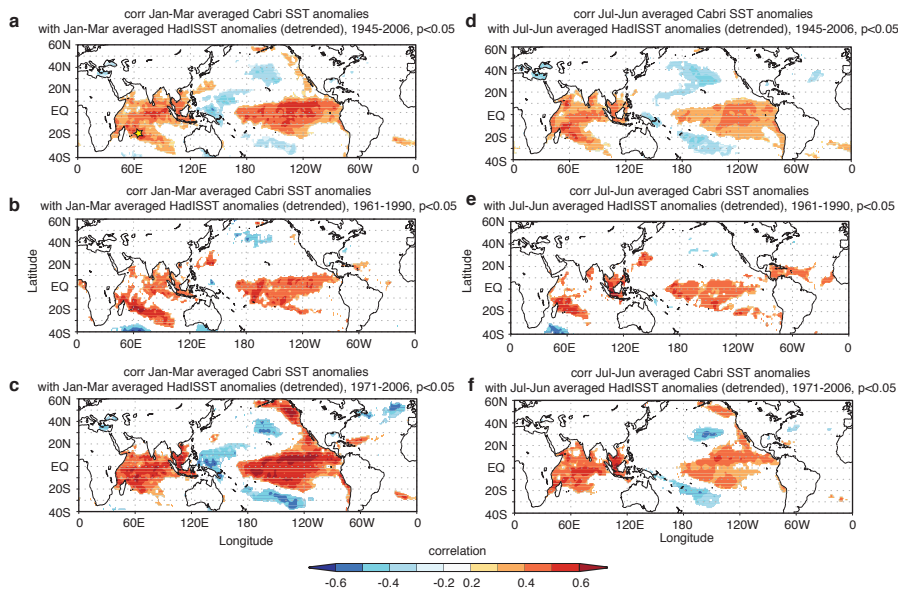
1133 Figure 5 – Time series of annual mean temperatures anomalies relative to the 1961-1990
 1134 mean for the coral Cabri SST reconstruction, Rodrigues weather station Air temperature
 1135 (AT), ERSSTv3b, ERSSTv4 , HadISST, HadSST3, HadMAT1 and HadNMAT2 for the
 1136 period 1950 to 2006. The uncertainty of mean annual coral Sr/Ca-SST anomalies are
 1137 indicated by the grey envelope.

1138

1139

1140





1143

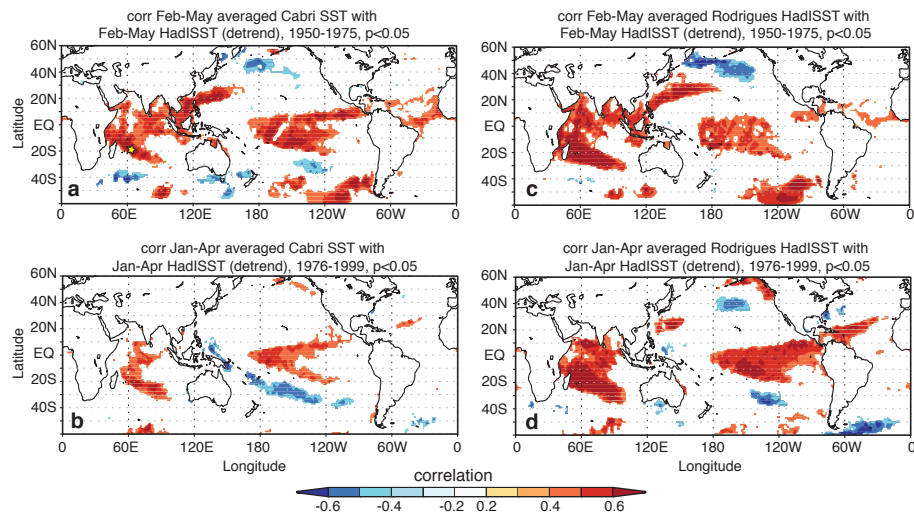
1144 | Figure 6 – Spatial correlation of Cabri Sr/Ca-SST anomalies (relative to 1961-1990) with
 1145 HadISST (Rayner et al., 2003). January to March austral summer in a) between 1945-
 1146 2006, b) 1961-1990 and c) 1971-2006. Annual mean correlations in d) between 1945-
 1147 2006, e) 1961-1990 and f) 1971-2006. Only correlation with $p < 0.05$ are coloured.
 1148 Computed at knmi climate explorer (van Oldenborgh and Burgers, 2005). Yellow star in
 1149 a) marks location of Rodrigues Island.

1150

1151

Jens Zinke 4/10/2016 4:04 PM

Deleted: 7



1153

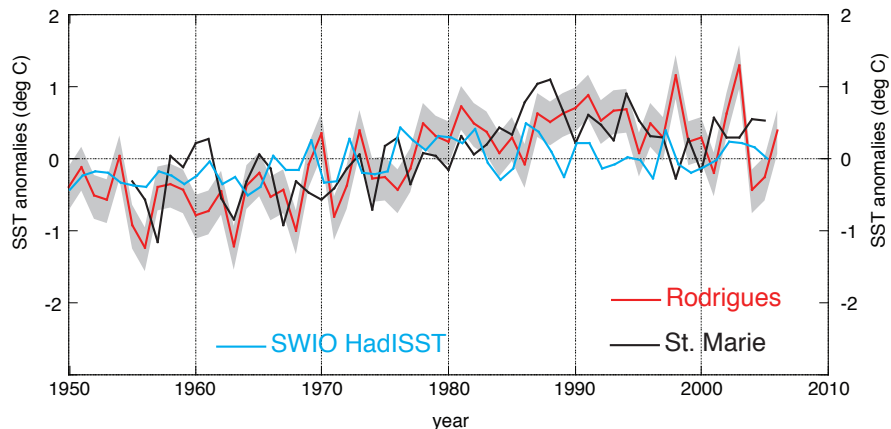
1154 | Figure 7 – Spatial correlations of Left) Cabri coral SST and Right) HadISST grid for
 1155 Rodrigues Island with global austral summer HadISST for a-c) 1950 to 1975 (February to
 1156 May) negative PDO phase (Mantua et al., 1997) and c-d) 1976 to 1999 (January to April)
 1157 positive PDO phase. Only correlations with $p < 0.05$ coloured. Computed at knmi climate
 1158 explorer (van Oldenborgh and Burgers, 2005). Yellow star in a) marks location of
 1159 Rodrigues Island.

1160

1161

Jens Zinke 4/10/2016 4:04 PM

Deleted: 8



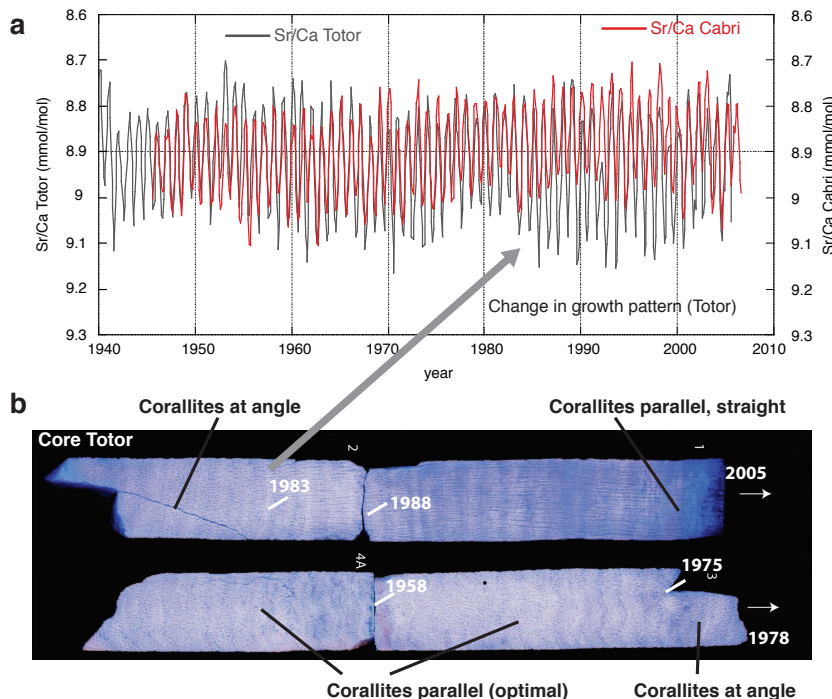
1163

1164 | Figure 8 – Comparison of southwestern Indian Ocean (SWIO) coral records from St.
 1165 | Marie Island (black; Grove et al., 2013) with the Cabri record from Rodrigues (red). An
 1166 | SST time series for the grid-box in the SWIO averaged between 12-20°S and 50-63°E is
 1167 | also illustrated (light blue). All time were annualized and converted to SST anomalies
 1168 | relative to 1961-1990. The uncertainty of mean annual Cabri Sr/Ca-SST anomalies are
 1169 | indicated by the grey envelope.

1170

Jens Zinke 4/10/2016 4:04 PM

Deleted: 9



1172

1173 Figure 9 – a) Monthly interpolated Sr/Ca profiles for cores Cabri (red).
 1174 B) Images of core Totor (coloured blue) with orientation of corallites indicated.
 1175 Years for core sections indicated on coral slab and grey arrow points to major change in orientation
 1176 of corallites in core top section of Totor around 1983/84.

1177

1178

1179

1180

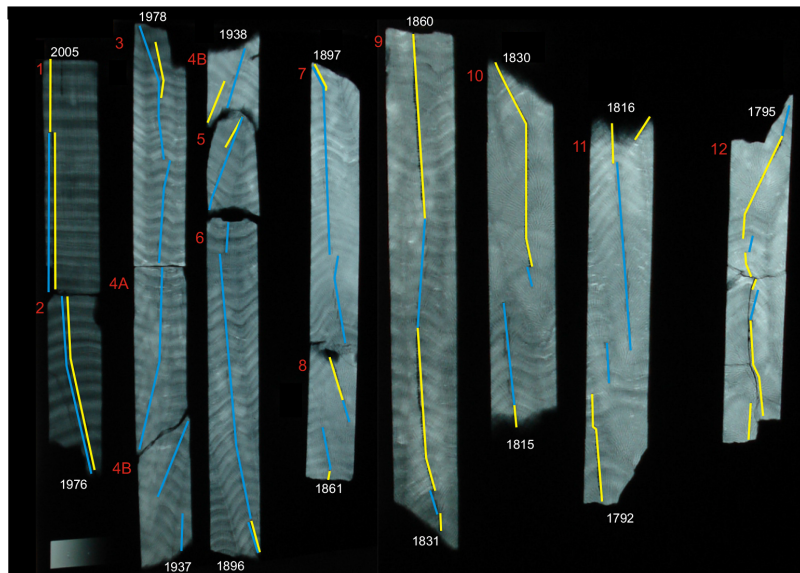
1181

1182

1183

1184 Appendix A –Instrumental sea surface temperature (SST) records and linear
1185 regression equations of coral Sr/Ca with SST.

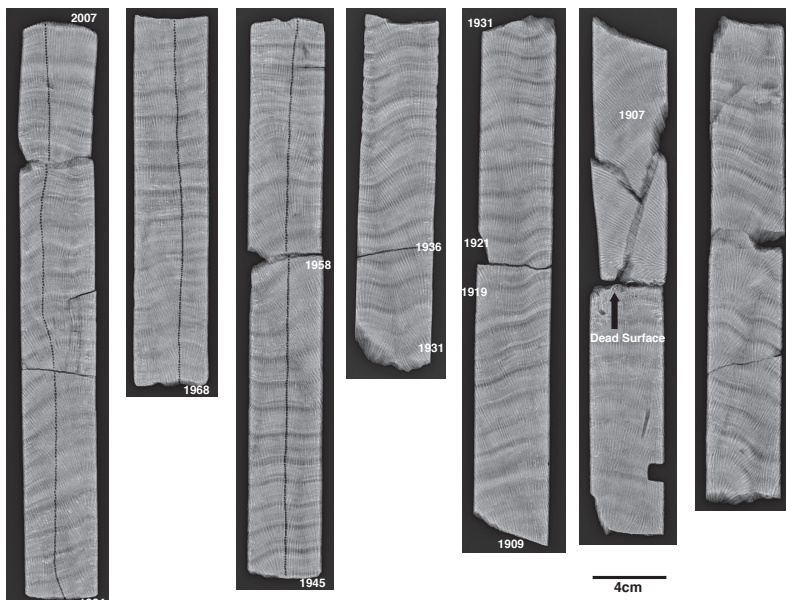
1186



1187

1188 Figure A1 – X-ray negative print for core sections of core Totor with sampling lines
1189 indicated. Blue lines indicate high resolution sampling tracks. Yellow lines superimposed
1190 on blue lines indicate sampling at annual resolution for other purposes. Start or end years
1191 for each core section indicated.

1192



1193

1194

Figure A2 - X-ray negative print for core sections of core Cabri with sampling lines

1195

(milling holes) indicated. Start or end years for each core section indicated. Note the dead

1196

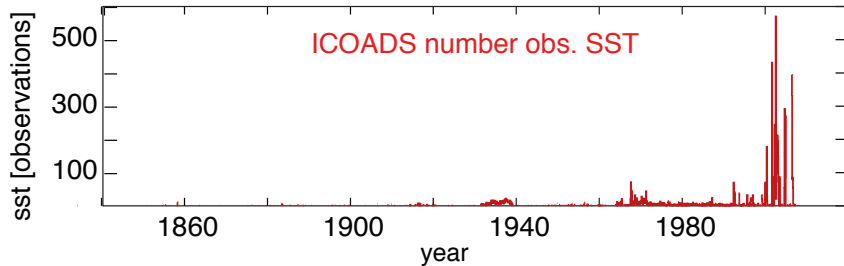
surface before 1907 that is most probably related to a past coral bleaching event.

1197

1198

1199

1200



1201

1202 | Figure A3 –Number of SST observations in the grid box surrounding Rodrigues in the
 1203 | ICOADS database. Note the extremely sparse observations even in recent years (van
 1204 | Oldenborgh and Burgers, 2005).

1205

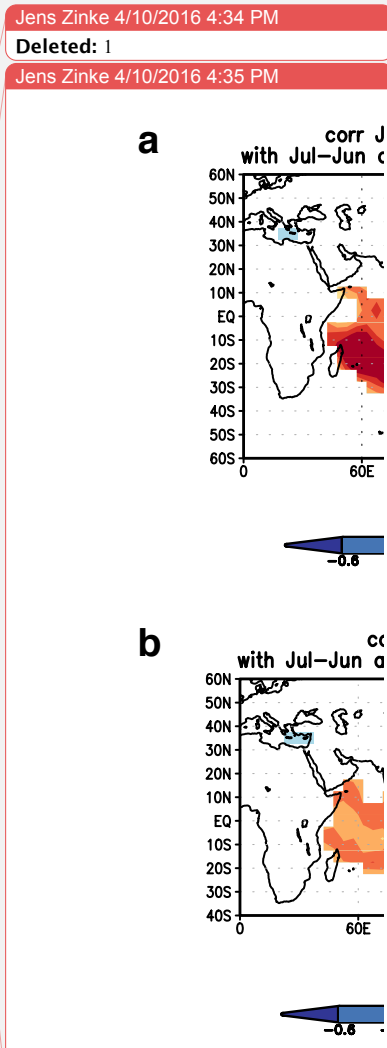
1206 |

1207 |

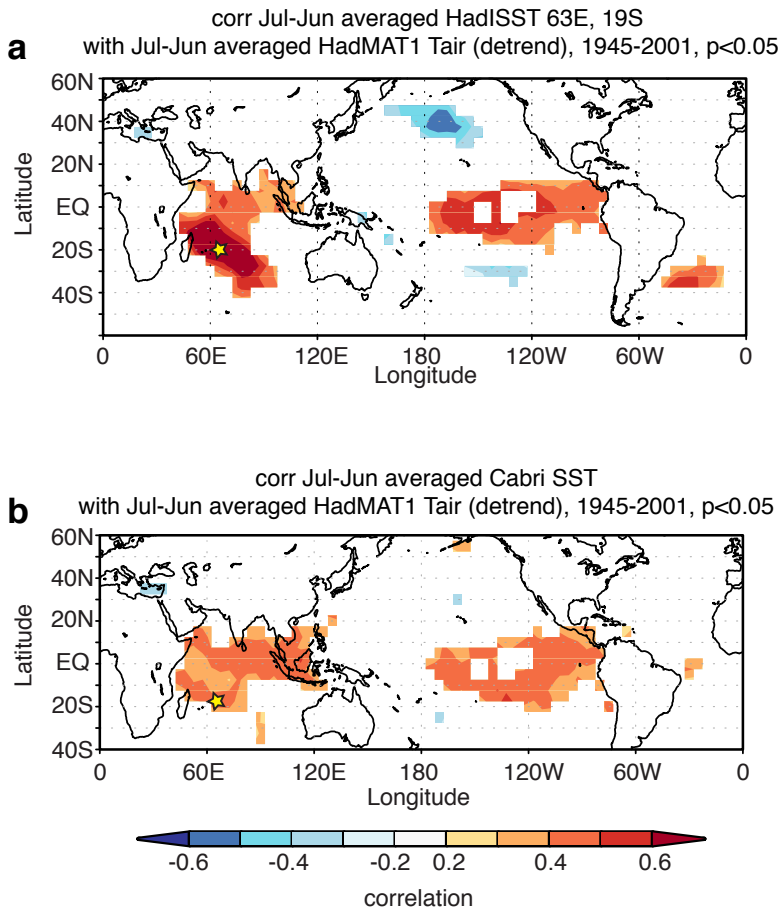
1208 |

1209 |

1210 |



Deleted:
 Jens Zinke 4/10/2016 4:35 PM
Deleted: Figure A2 – Spatial correlations of mean annual HadMAT1 air temperature anomalies between 1945 to 2001 relative to 1961-1990 with a) HadISST for Rodrigues, and b) Cabri SST. Only correlations with $p < 0.05$ coloured. Computed at knmi climate explorer (van Oldenborgh and Burgers, 2005). Y-axis Latitude, X-axis Longitude.

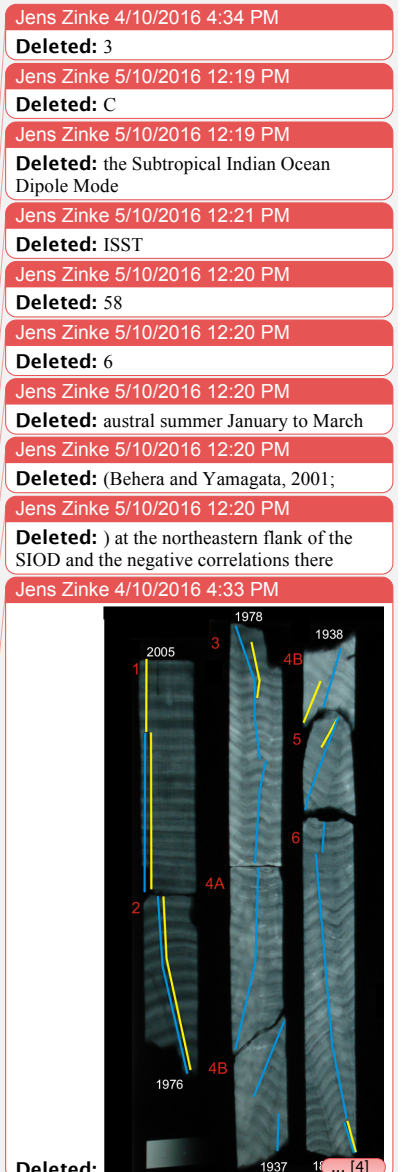


1221

1222 Figure A4 – **a**) Spatial correlation of HadISST for the grid box of Rodrigues Island with
 1223 global HadMAT1 marine air temperature, (Tair) between 1945 and 2001 for July to June
 1224 annual averages (Rayner et al., 2003). Note the location of Rodrigues Island marked by
 1225 yellow star, **b**) same as a), but for Cabri SST with global HadMAT1. Only correlations
 1226 with $p<0.05$ coloured. Computed at knmi climate explorer (van Oldenborgh and Burgers,
 1227 2005).

1228

1229



	SST <i>in situ</i> 2002-2006	AVHRR SST 2002-2006	ERSST 2002-2006	Air Temp. 2002-2006
Mean annual	25.49 (0.24)	25.4 (0.11)	25.57 (0.3)	27.49 (0.31)
Maximum	28.6 (0.5)	28.65 (0.44)	28.29 (0.4)	31.2 (0.62)
Minimum	22.4 (0.27)	22.75 (0.21)	23.15 (0.13)	24.2 (0.44)
Seasonal Range	6.22 (0.68)	5.9 (0.58)	5.14 (0.39)	7.0 (0.79)
STDV	2.14	1.78	1.69	2.07

1243

1244 Table A1 – Statistics of various sea surface temperature (SST) products and air
 1245 temperature for Rodrigues with 1σ standard deviations in brackets for the period 2002 to
 1246 2006 (period with *in situ* SST data). STDV = 1σ standard deviation over all years. All
 1247 units in °C.

1248

1249

1250

1251

1252

1253

1254

1255

1256

1257

1258

(a) Max-Min	Regression equation	r^2	p
Totor	Sr/Ca = -0.0439(± 0.004)*SST + 10.032(± 0.10)	0.97	<0.001
Cabri	Sr/Ca = -0.0384(± 0.005)*SST + 9.861(± 0.12)	0.89	<0.001
(b) Max-Min			
Totor	Sr/Ca = -0.0638(± 0.004)*SST + 10.566(± 0.09)	0.95	<0.001
Cabri	Sr/Ca = -0.0507(± 0.004)*SST + 10.179(± 0.10)	0.90	<0.001
(c) Max-Min			
Totor	Sr/Ca = -0.0531(± 0.004)*SST + 10.271(± 0.11)	0.96	<0.001
Cabri	Sr/Ca = -0.0441(± 0.005)*SST + 10.012(± 0.13)	0.88	<0.001
(d) Monthly			
Totor	Sr/Ca = -0.0522(± 0.003)*SST + 10.272(± 0.08)	0.79	<0.001
Cabri	Sr/Ca = -0.0419(± 0.003)*SST + 9.95(± 0.07)	0.87	<0.001

1259

1260 Table A2 - Linear regression of coral Sr/Ca with a) *in situ* SST 2002-2005/6, b)
 1261 ERSSTv.3 (Smith et al., 2008) 1997-2005/6, c) AVHRR SST NOAA Coral Reef watch
 1262 data 2000-2005/6 and d) monthly Sr/Ca with AVHRR SST (Reynolds et al., 2007) for the
 1263 period 1982 to 2005.

1264
 1265